

CHAPTER 4

NUMERICAL EXAMPLES

4.1 General

To evaluate the reliability of the proposed concept and to demonstrate the implementation procedure, SDOF (Single-Degree-of-Freedom) and MDOF (Multi-Degree-of-Freedom) systems are employed here with different types of nonlinearity. Nonlinear conservative as well as non-conservative systems are tested. The mechanical models representing systems, as described in 3.2, are subjected to base excitations. The data sets which are used in the training and testing procedures are obtained from the numerical integration of the hybrid discrete-ANNs systems using those based excitations.

4.2 Description of Excitation

Two different excitations are employed in the numerical examples. The first one is based on mathematical model known as the Kanai-Tajimi model (Kanai 1957) and (Tajimi 1960). The second one is the scaled EI-Centro North-South component (Chopra 2001).

4.2.1 Kanai-Tajimi (KT) seismic model

The Kanai-Tajimi model is a non-stationary white noise process, obtained from a filtered white noise process with a modulation function. The filter employs the modified Kanai-Tajimi model, which has the filter equation as (Schuëller et al. 1998)

$$\begin{bmatrix} \dot{Y}_1 \\ \dot{Y}_2 \\ \dot{Y}_3 \\ \dot{Y}_4 \end{bmatrix} = \begin{bmatrix} 0 & 1 & 0 & 0 \\ -\Omega_{1g}^2 & -2\zeta_{1g}\Omega_{1g} & 0 & 0 \\ 0 & 0 & 0 & 1 \\ \Omega_{1g}^2 & 2\zeta_{1g}\Omega_{1g} & -\Omega_{2g}^2 & -2\zeta_{2g}\Omega_{2g} \end{bmatrix} \begin{bmatrix} Y_1 \\ Y_2 \\ Y_3 \\ Y_4 \end{bmatrix} + \begin{bmatrix} 0 \\ W(t) \\ 0 \\ 0 \end{bmatrix} \quad (4.1)$$

where $W(t)$ is a stationary Gaussian white noise process with 2-side power spectral G_0 . The ground acceleration A_g is defined as:

$$A_g(t) = g(t) [\Omega_{1g}^2 Y_1(t) + 2\zeta_{1g}\Omega_{1g} Y_2(t) - \Omega_{2g}^2 Y_3(t) - 2\zeta_{2g}\Omega_{2g} Y_4(t)] \quad (4.2)$$

in which $g(t)$ is a temporal modulation function.

To account for the non-stationary characteristics of earthquake excitation, the temporal modulation $g(t)$ as proposed by (Amin & Ang 1968) is applied

$$g(t) = \begin{cases} 0 & t \leq 0 \\ (t/t_1)^2 & 0 < t \leq t_1 \\ 1 & t_1 < t \leq t_2 \\ \exp(-c_\phi(t-t_2)) & t > t_2 \end{cases} \quad (4.3)$$

in which t_1 , t_2 , and c_ϕ are the model parameters. All utilized parameters of the Kanai-Tajimi model are shown in Tables 4.1 and 4.2. The digital data of these earthquake records, i.e. A_{g1} and A_{g2} are tabulated in Appendix A and B, respectively.

Table 4.1 Parameters used for simulation of A_{g1} according to the KT model

Parameter (unit)	Value
G_0	3.00
ζ_{1g}	0.600
Ω_{1g} (rad/s)	9.26
ζ_{2g}	0.313
Ω_{2g} (rad/s)	19.0
t_1 (s)	5.00
t_2 (s)	10.0
c_ϕ	0.7



Fig. 4.1 Simulated ground acceleration A_{g1} according to KT model

Table 4.2 Parameters used for simulation of A_{g2} according to the KT model

Parameter (unit)	Value
G_0	1.00×10^{-2}
ζ_{1g}	0.600
Ω_{1g} (rad/s)	9.26
ζ_{2g}	0.313
Ω_{2g} (rad/s)	19.0
t_1 (s)	4.00
t_2 (s)	10.0
c_ϕ	0.583

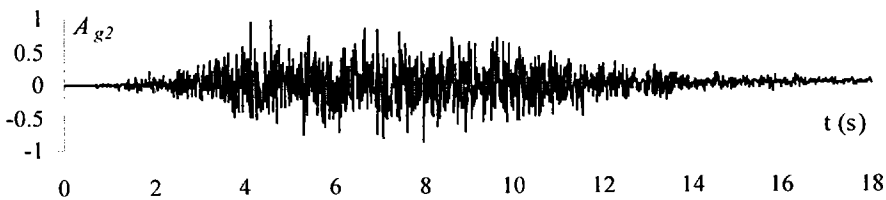


Fig. 4.2 Simulated ground acceleration A_{g2} according to KT model

4.2.2 EI-Centro earthquake ground motion

The North-South EI-Centro is the ground acceleration history recorded at a site in EI Centro, California, during the Imperial Valley, California, earthquake of May 18, 1940. In present case, the Scaled EI-Centro earthquake is scaled to be the history A_{g3} . The digitized values can be found in Appendix C.

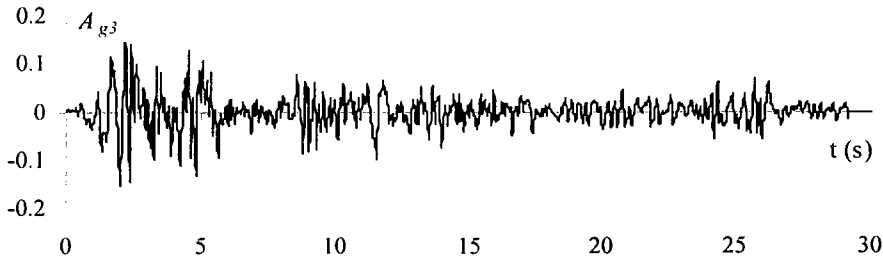


Fig. 4.3 Scaled EI-Centro ground acceleration A_{g3}

4.3 Simulation of Training and Testing Data

From Eq. (3.2), one can rewrite equation of motion at a time instant t_i

$$f_{R,t_i} = P_{ext,t_i} - m\ddot{u}_{t_i}. \quad (4.4)$$

This means that the restoring force at the time t_i is always available if the corresponding external force and acceleration are measurable. It is assumed in all following examples that those two values are measurable. In addition, the system responses, i.e. the displacement and velocity are as assumed such that as well.

4.4 Nonlinear Conservative SDOF System

The conservative system, namely Duffing system, is considered here. The non-linearity belongs to the hardening type.

$$m\ddot{u} + c\dot{u} + k_1u + k_2u^3 = -mA_g \quad (4.5)$$

where c , k_1 , k_2 , are damping, linear stiffness, and nonlinear stiffness of this system. The spring force is described by,

$$f_s = k_1u + k_2u^3. \quad (4.6)$$

The initial condition of this system, i.e. u_0 , \dot{u}_0 , \ddot{u}_0 , are all zero. The following table shows the system properties.

Table 4.3 Parameters in Duffing (hardening-type) system

Parameter (unit)		Value
m	kg	50,000
c	Ns/m	65,900
k_1	N/m	24,200,000
k_2	N/m	1,000,000

1) Selection a network inputs

The non-linear restoring force is modeled by the ANNs-based model. For the Duffing oscillation, the network architecture is shown in Fig. 4.4.

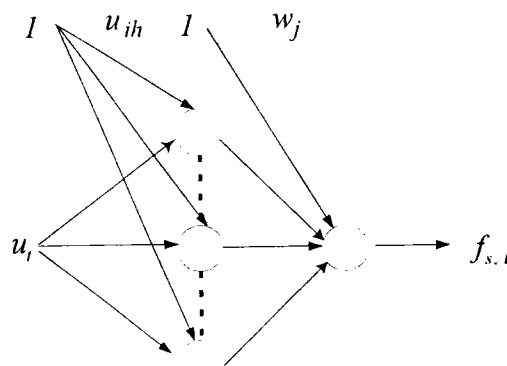


Fig. 4.4 Architecture of ANNs for modeling of Duffing Oscillator

The corresponding functional form of the ANNs is

$$f_{ANN,t} = ANN(u_i). \quad (4.7)$$

2) Training the network

The first earthquake record, A_{g1} , is used as the training data set. The total duration for training time histories is 20 seconds from which the input values are extracted from the time histories and fed into the network at every 0.01-second. Only known damping case is considered.

From parametric study, the one hidden layer neural network and 10 hidden neurons yield satisfactory results. The corresponding optimal weights for this duffing system are given in Appendix D.

The exact results, or computed from Eq. (4.5), is compared with those from ANNs, as shown in Figs. 4.5, 4.6 and 4.7.

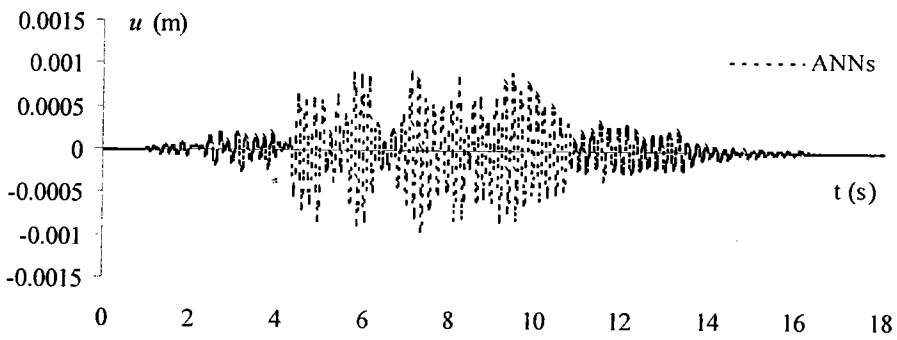
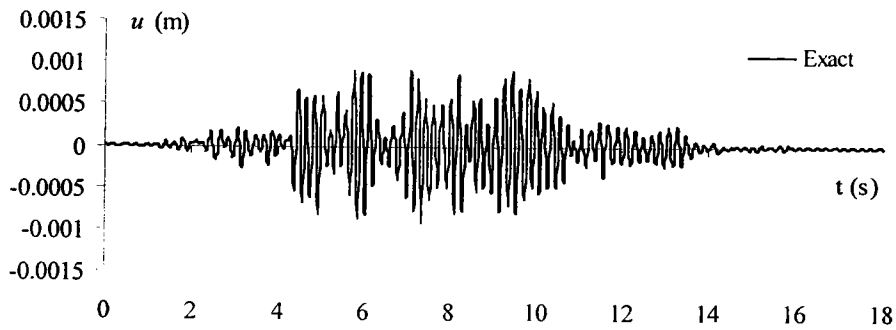


Fig. 4.5 Displacement resulting from the first ground acceleration A_{g1}

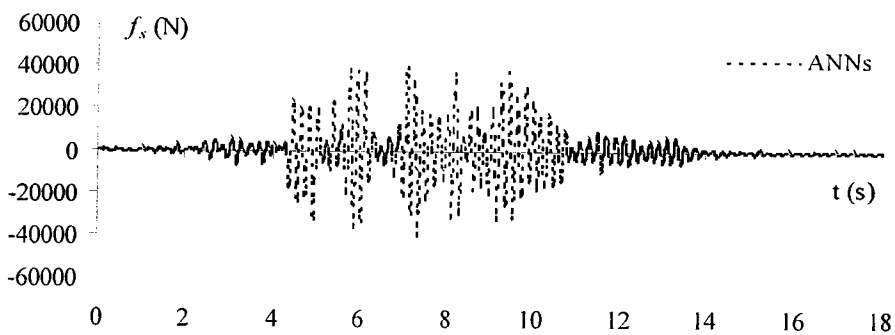
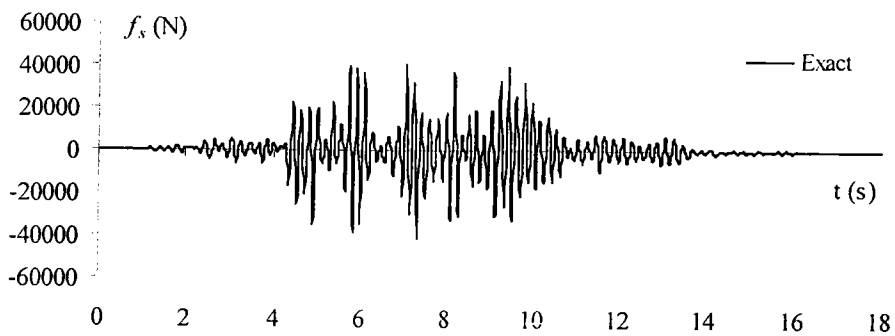


Fig. 4.6 Spring force resulting from the first ground acceleration A_{g1}

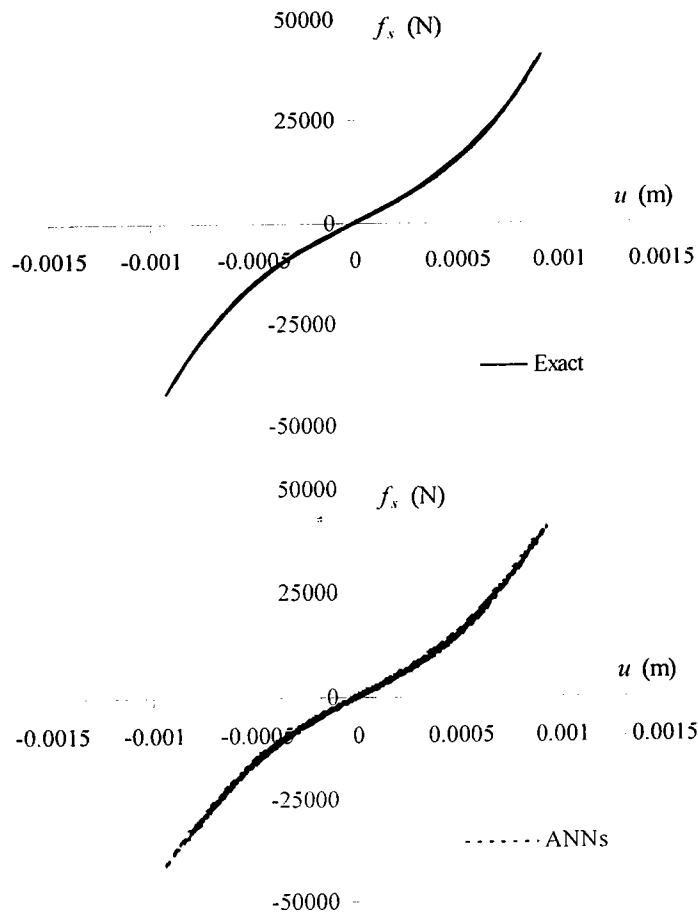


Fig. 4.7 Spring force-Displacement relation from the first ground acceleration A_{g1}

3) Testing the trained network

The predicted responses of this system from the trained ANN using the second ground acceleration record, A_{g2} are shown in Figs. 4.8 – 4.10. Some discrepancy appears in the relation of second seismic response. The reason is that the domain where the discrepancy happens is considerably beyond the domain of the training data. Nevertheless, this characteristic does not significantly affect the accuracy of the response.

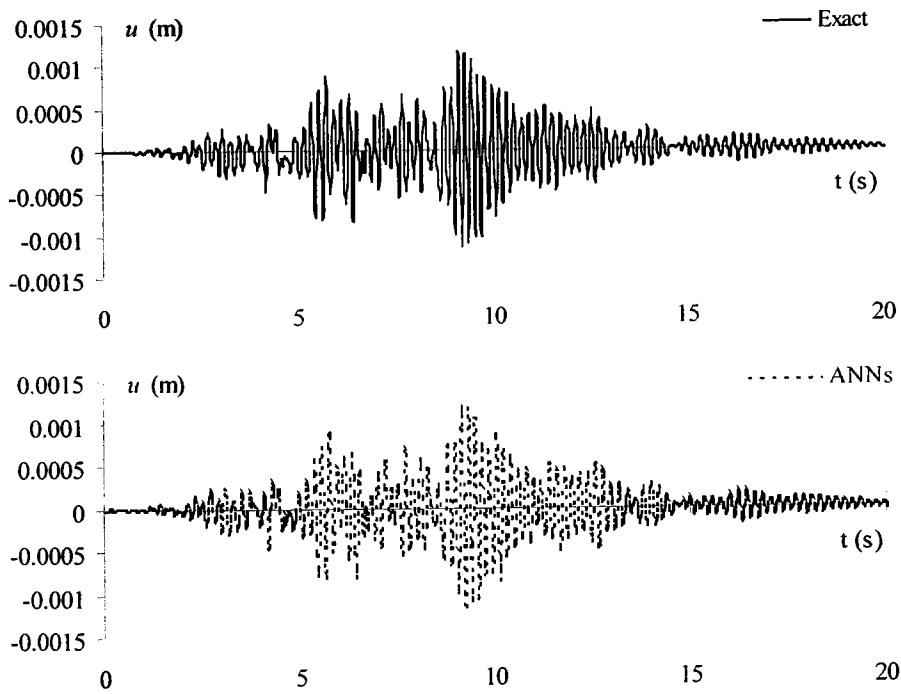


Fig. 4.8 Displacement resulting from the second ground acceleration A_{g2}

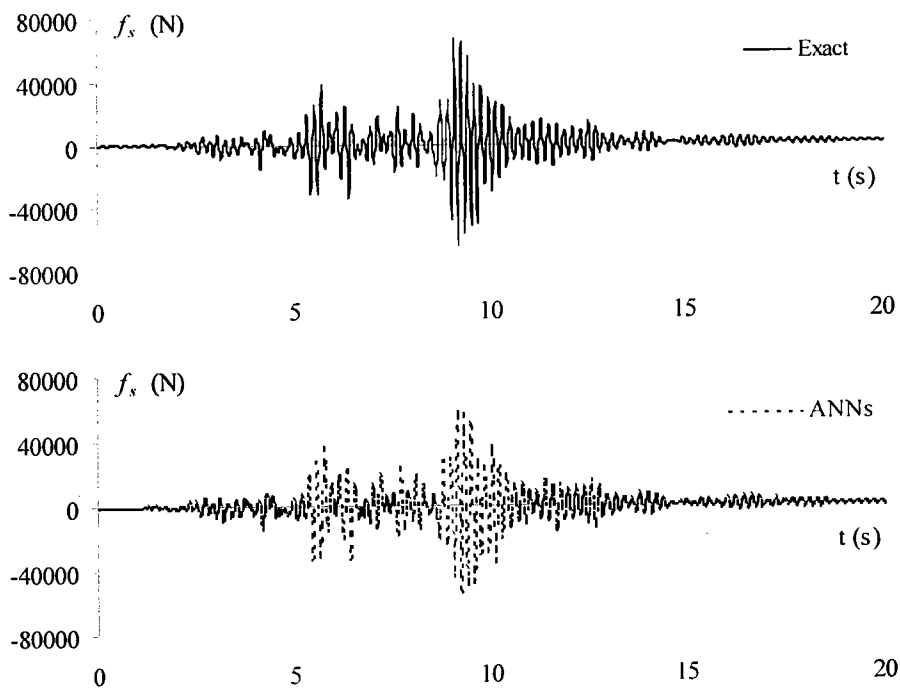


Fig. 4.9 Spring force resulting from the second ground acceleration A_{g2}

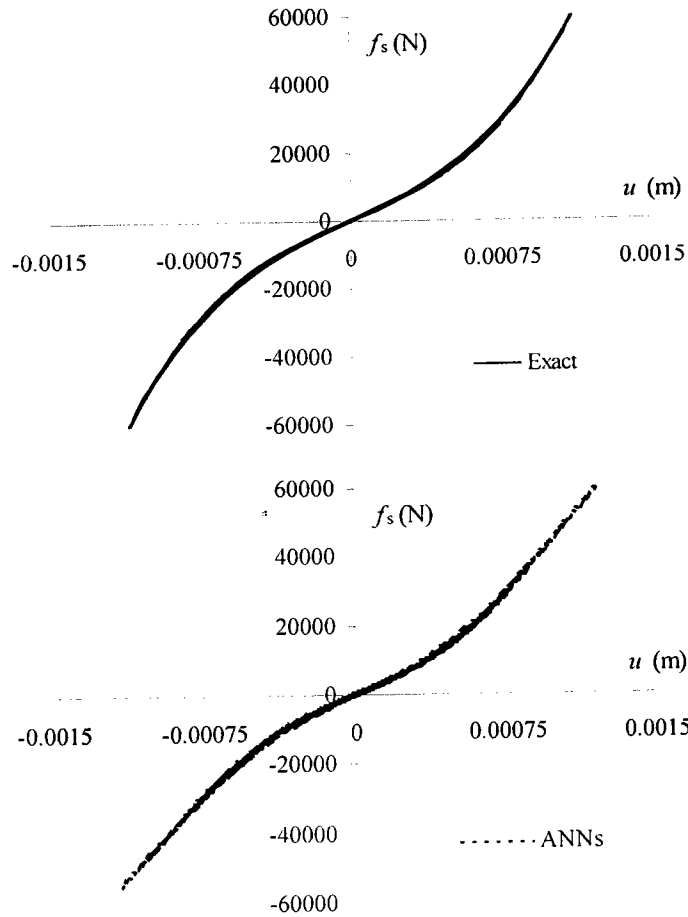


Fig. 4.10 Spring force-Displacement relation from the second ground acceleration A_{g2}

4.5 Nonlinear Non-Conservative SDOF System

4.5.1 Clough-Johnston (CJ) hysteretic system

The Clough-Johnston hysteretic model (Clough and Johnston 1966) was originally designed for RC beam-columns. The differential description of the model was first introduced by Minai and Suzuki (1985). The equation of motion for this system is:

$$m \ddot{u} + c \dot{u} + \alpha k_1 u + (1 - \alpha) k_1 Z = -m A_g \quad (4.8)$$

$$g(\dot{u}, Z; Z_Y) = H(\dot{u})H(Z - Z_Y) - H(-\dot{u})H(-Z - Z_Y) \quad (4.9)$$

$$\dot{Z} = f(\dot{u}, Z, D; Z_Y) \dot{u} \quad (4.10)$$

$$\dot{D} = g(\dot{u}, Z; Z_Y) \dot{u} \quad (4.11)$$

$$f(u, Z, D; Z_Y) = H(Z) \{ AH(\dot{u})(1 - H(Z - Z_Y)) + H(-\dot{u}) \} \\ + H(-Z) \{ AH(-\dot{u})(1 - H(-Z - Z_Y)) + H(\dot{u}) \} \quad (4.12)$$

$$H(X) = \begin{cases} 1 & , u \geq 0 \\ 0 & , u < 0 \end{cases} \quad (4.13)$$

$$A = \frac{Z_Y}{Z_Y + D} \quad (4.14)$$

in which all system parameters i.e., m , c , k_l , u are the same as duffing case. α determines the elastic fraction in the total spring force. Z is the hysteretic displacement. The Clough-Johnston model represents the elasto-plastic constitutive law with stiffness degradation, in which Z_Y denotes the yield level. The damage level D is designated as the accumulated plastic deformation of the hysteretic element. The spring force, f_s , is combined with linear, $\alpha k_l X$, and nonlinear part, $(1 - \alpha) k_l Z$. It can be seen that the higher α value is, the more linear proportion takes part in the restoring force. Two cases of α are considered here, namely $\alpha = 0.1$ and 0.3 . Table 4.4 and 4.5 show the system parameters used in this study. The dynamical system above is subjected to the following initial conditions:

$$u(0) = u_o, \dot{u}(0) = 0, \ddot{u}(0) = 0 \quad (4.15)$$

$$Z(0) = Z_o \quad (4.16)$$

$$D(0) = D_o. \quad (4.17)$$

The system with existing damage can be simulated with the system of equations above by setting the non-zero initial conditions in Eq. (4.15) to Eq. (4.17). It is assumed that there exist initial damages to the system before being exposed to the first ground acceleration, A_{g1} . After the first earthquake excitation for 19 seconds, the second seismic, A_{g2} , interact with the same system this condition is used for the least of this CJ hysteretic system.

1) Case of $\alpha = 0.3$ and known damping

Consider Eq. (4.8),

$$m \ddot{u} + c \dot{u} + \alpha k_l u + (1 - \alpha) k_l Z = -m A_g. \quad (4.18)$$

Here the spring force,

$$f_s = \alpha k_l u + (1 - \alpha) k_l Z, \quad (4.19)$$

is assumed unknown and modeled by ANNs. That is

$$m \ddot{u} + c \dot{u} + f_{ANN} = -m A_g. \quad (4.20)$$

Table 4.4 shows the parameters used in this case.

Table 4.4 Parameters used in Clough-Johnston hysteretic model ($\alpha = 0.3$)

Parameter (unit)		Value
m	kg	50,000
c	Ns/m	65,900
k_I	N/m	24,200,000
Z_Y	m	0.00015
α		0.3
D_o	m	-0.00114
Z_o	m	0
u_0	m	0
\dot{u}_0	m/s	0
\ddot{u}_0	m/s ²	0

1.1) Selection a network inputs

As described in section 3.4, nonlinear restoring force of non-conservative system was dependent on past response history. Correspondingly, the input parameters for predicting nonlinear restoring force are

$$y = [u, u_{t-1}, u_{t-2}, \dot{u}, \dot{u}_{t-1}, \dot{u}_{t-2}, f_{R,t-1}, f_{R,t-2}]. \quad (4.21)$$

The architecture of ANNs is depicted in Fig. 4.11.

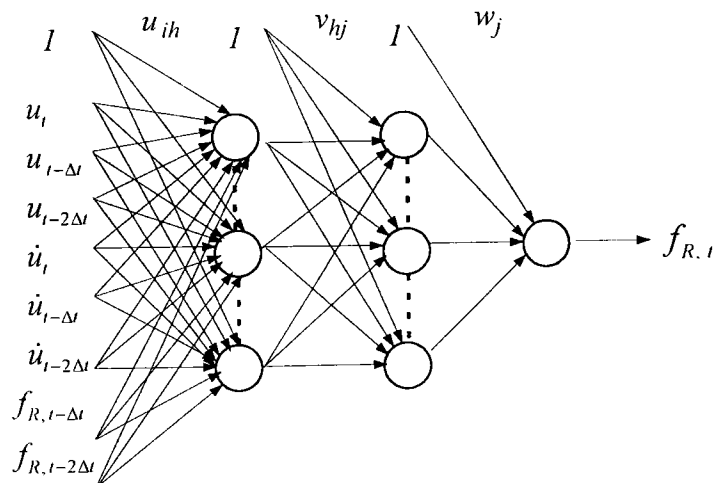


Fig. 4.11 Architecture of ANNs for modeling hysteretic restoring force

From the ANNs architecture and input-output variables, the proposed ANNs belong to the class of dynamic or recurrent neural networks. This type of input for the above-mention CJ hysteretic system will be used through the rest of the examples.

1.2) Training the network

The first earthquake record, A_{g1} , is used as the training data set. The training data are using simulated response of A_{g1} for 20 seconds and fed into the network every 0.01-second.

From parametric study, the two hidden layer neural network with 16-16 hidden neurons yields satisfactory results. The learning rate is 0.1 and training for 5115 epochs. The corresponding optimal weights for this system are given in Appendix E.

The exact results, or computed from Eq. (4.18), is compared with those from ANNs, as shown in Figs. 4.12, 4.13 and 4.14.

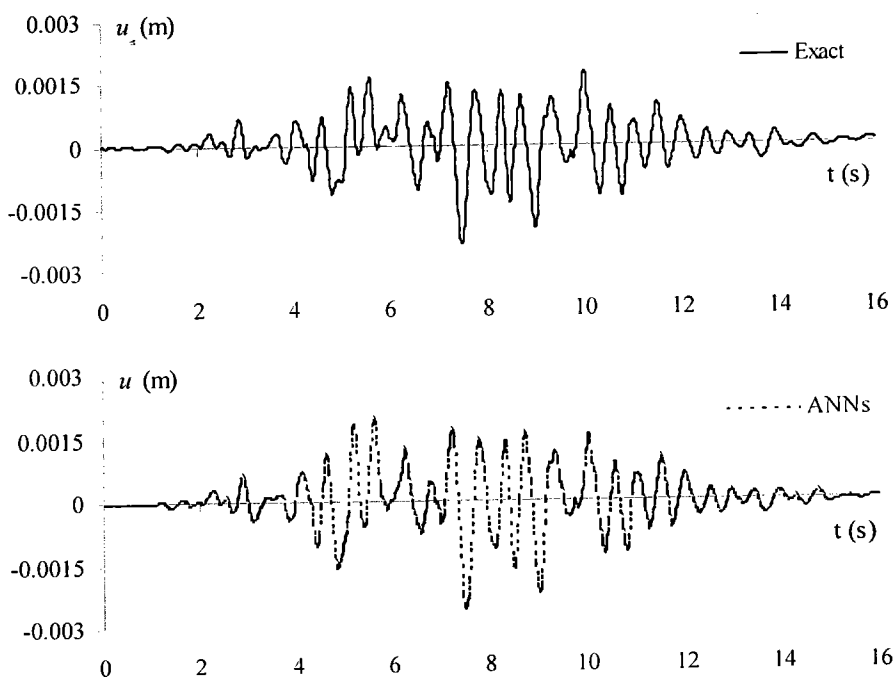


Fig. 4.12 Displacement resulting from the first ground acceleration A_{g1}

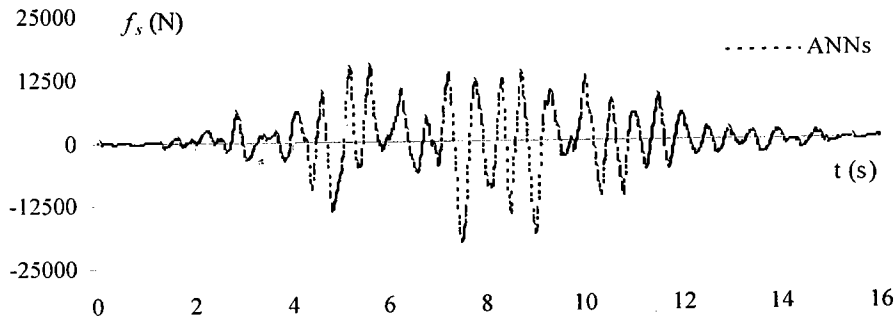
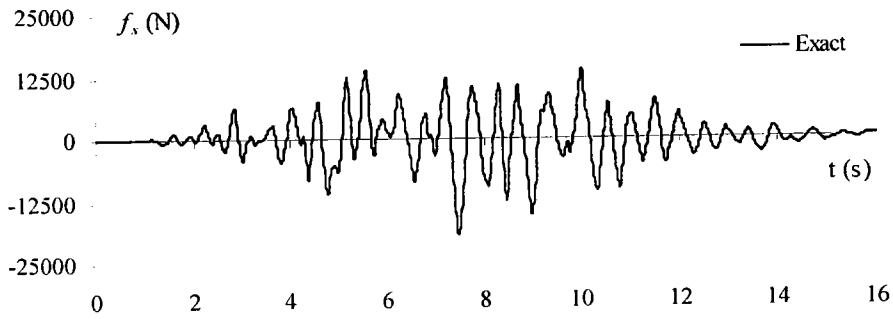


Fig. 4.13 Spring force resulting from the first ground acceleration A_{g1}

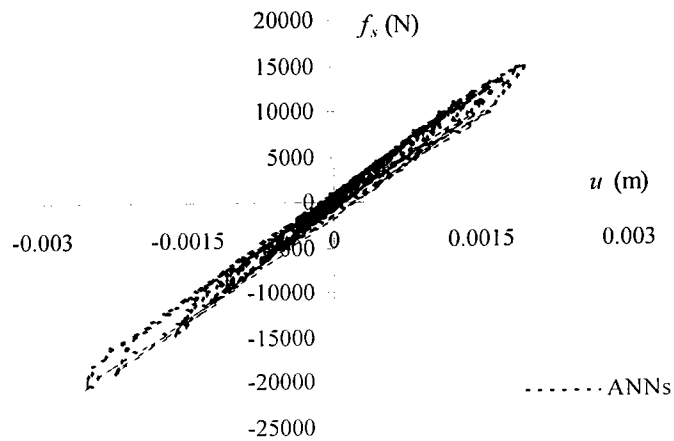
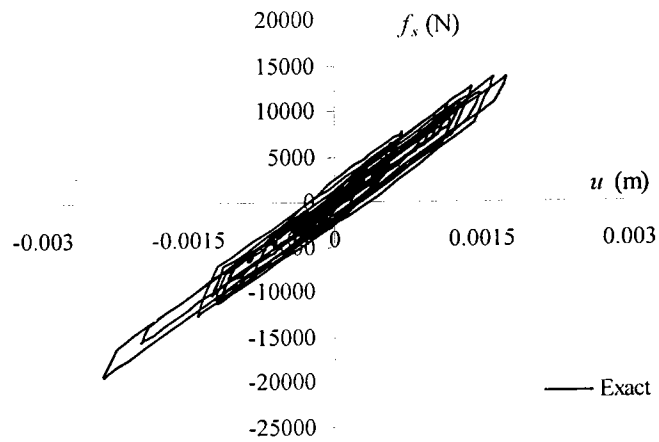


Fig. 4.14 Spring force-Displacement relation from the first ground acceleration A_{g1}

1.3) Testing the trained network

The predicted responses of this system from the trained ANN using the second ground acceleration record, A_{g2} are shown in Figs. 4.15 – 4.17.

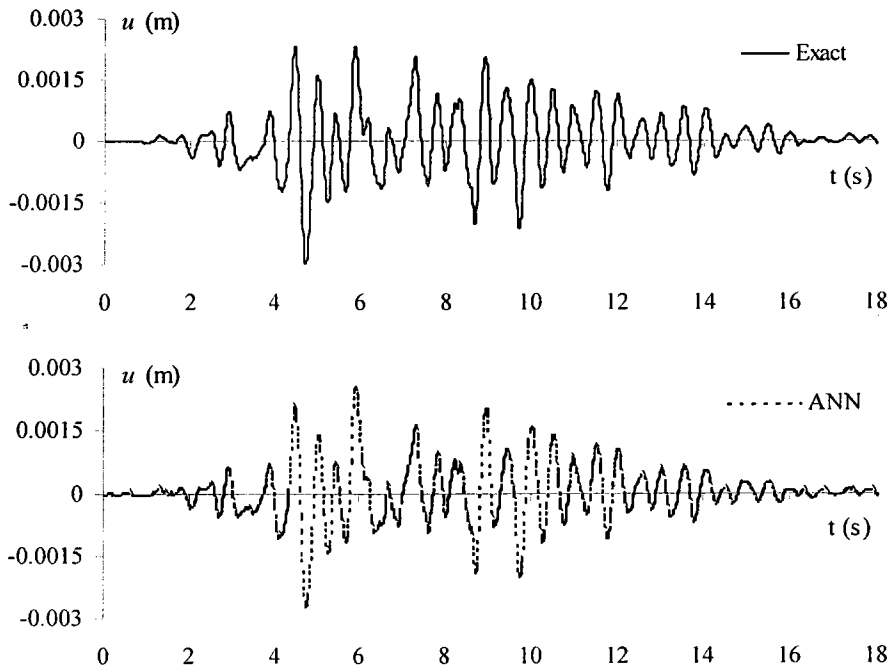


Fig. 4.15 Displacement resulting from the second ground acceleration A_{g2}

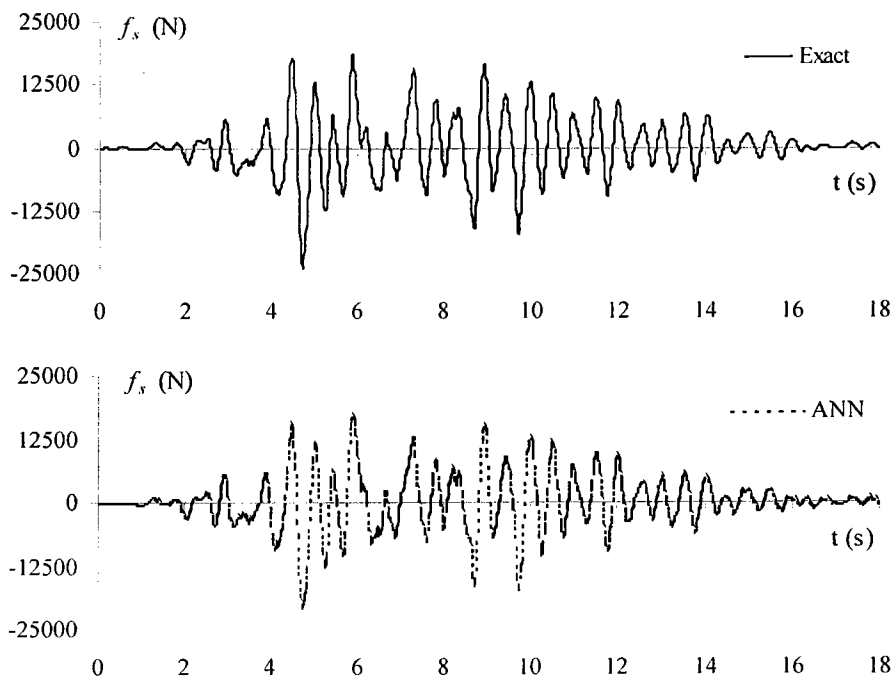


Fig. 4.16 Spring force resulting from the second ground acceleration A_{g2}

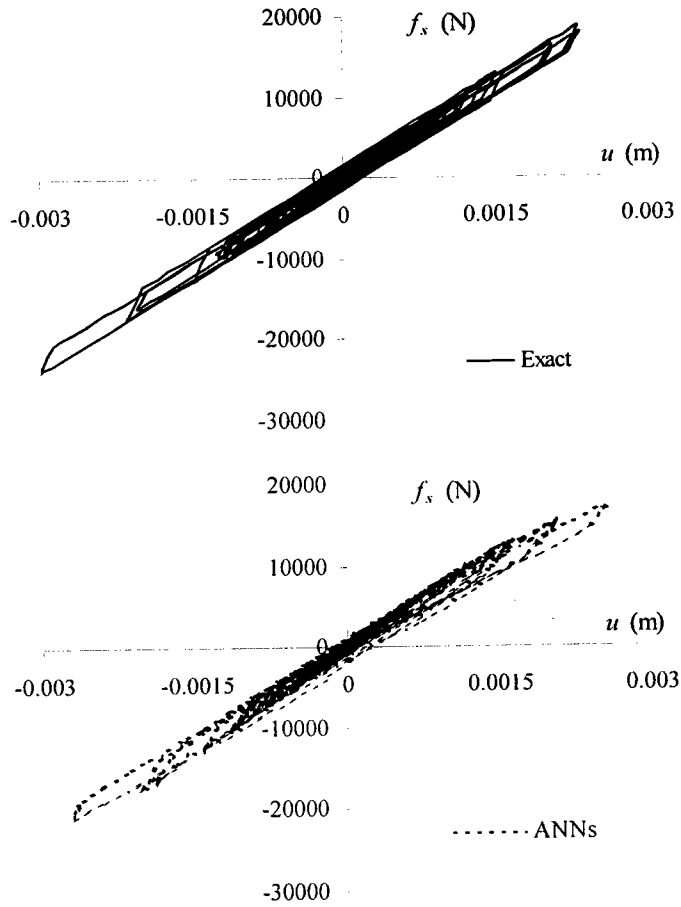


Fig. 4.17 Spring force-Displacement relation from the second ground acceleration A_{g2}

2) Case of $\alpha = 0.3$ and unknown damping

The equation of motion of CJ Hysteretic system, Eq. (4.8), is repeated:

$$m \ddot{u} + c \dot{u} + \alpha k_1 u + (1 - \alpha) k_1 Z = -m A_g . \quad (4.22)$$

Here the restoring force,

$$f_R = c \dot{u} + \alpha k_1 u + (1 - \alpha) k_1 Z , \quad (4.23)$$

is assume as unknown and modeled by ANNs. That is

$$m \ddot{u} + f_{ANN} = -m A_g . \quad (4.24)$$

This system is the same as known damping case.

2.1) Selection a network input

As described in section 3.4, Nonlinear restoring force of Non-conservative system was predicted dependent on past response history. From Eq. (3.12) the input parameters for predicting nonlinear restoring force are

$$y = [u, u_{i-1}, u_{i-2}, \dot{u}, \dot{u}_{i-1}, \dot{u}_{i-2}, f_{R,i-1}, f_{R,i-2}]. \quad (4.25)$$

2.2) Training the network

The first earthquake record, A_{g1} , is used as the training data set. The total duration for training time histories is 20 seconds from which the input values are extracted from the time histories and fed into the network at every 0.01-second.

From parametric study, the two hidden layer neural network and 24-24 hidden neurons yield satisfactory results. The learning rate is 0.1 and training for 19000 epochs. The corresponding optimal weights for this duffing system are given in Appendix F.

The exact results, or computed from Eq. (4.22), is compared with those from ANNs, as shown in Figs. 4.18, 4.19 and 4.20.

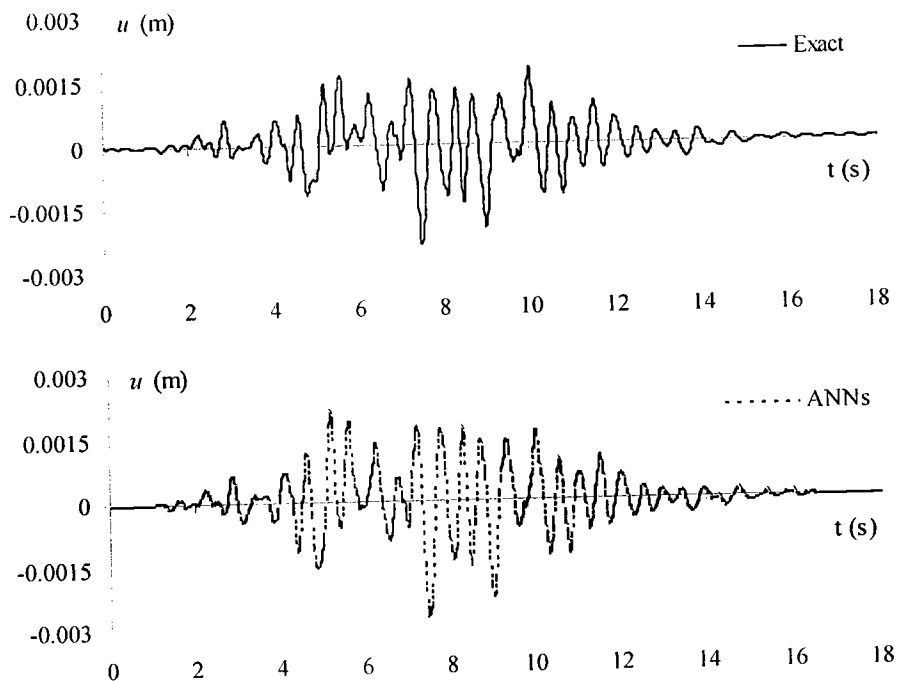


Fig. 4.18 Displacement resulting from the first ground acceleration A_{g1}

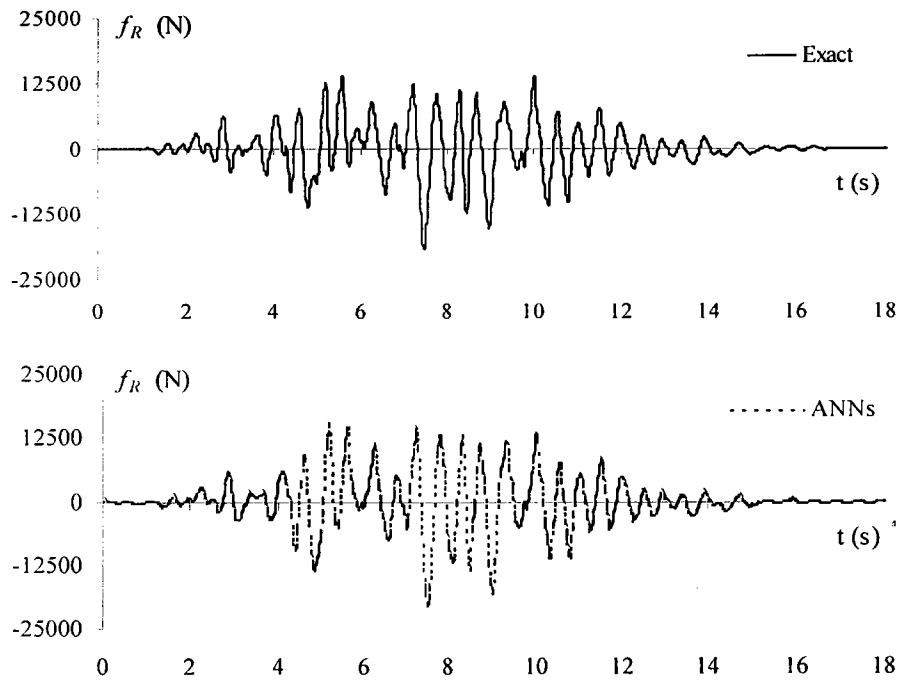


Fig. 4.19 Restoring force resulting from the first ground acceleration A_{g1}

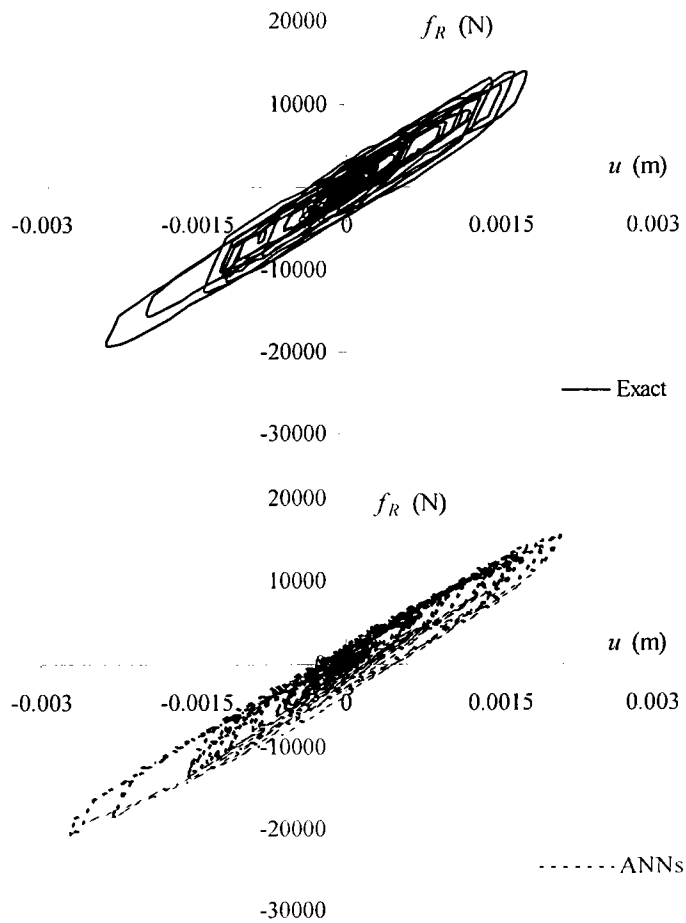


Fig. 4.20 Restoring force-Displacement Relation from the first ground acceleration A_{g1}

2.3) Testing the trained network

The predicted responses of this system from the trained ANN using the second ground acceleration record, A_{g2} are shown in Figs. 4.21 – 4.23.

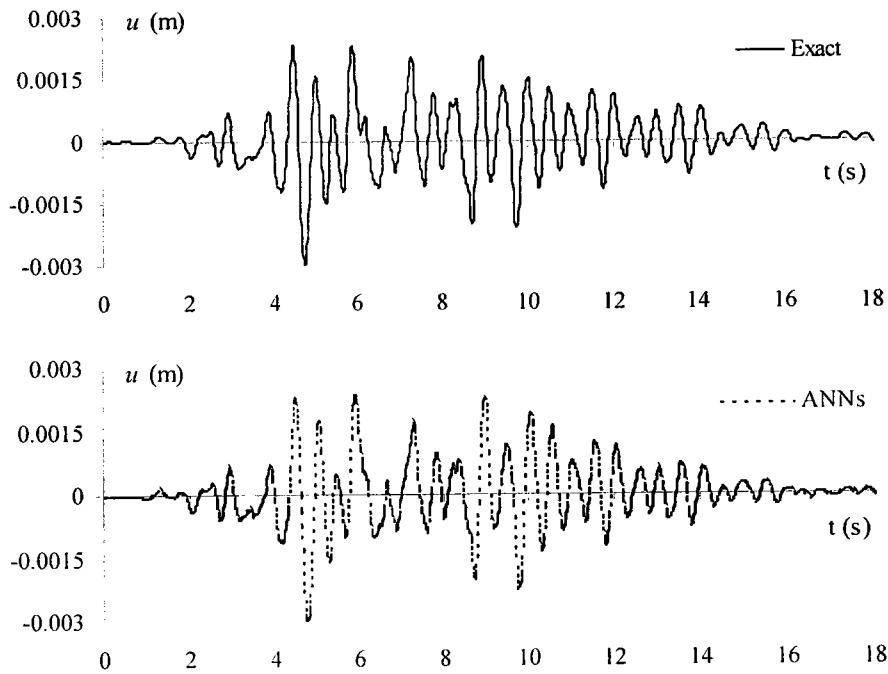


Fig. 4.21 Displacement resulting from the second ground acceleration A_{g2}

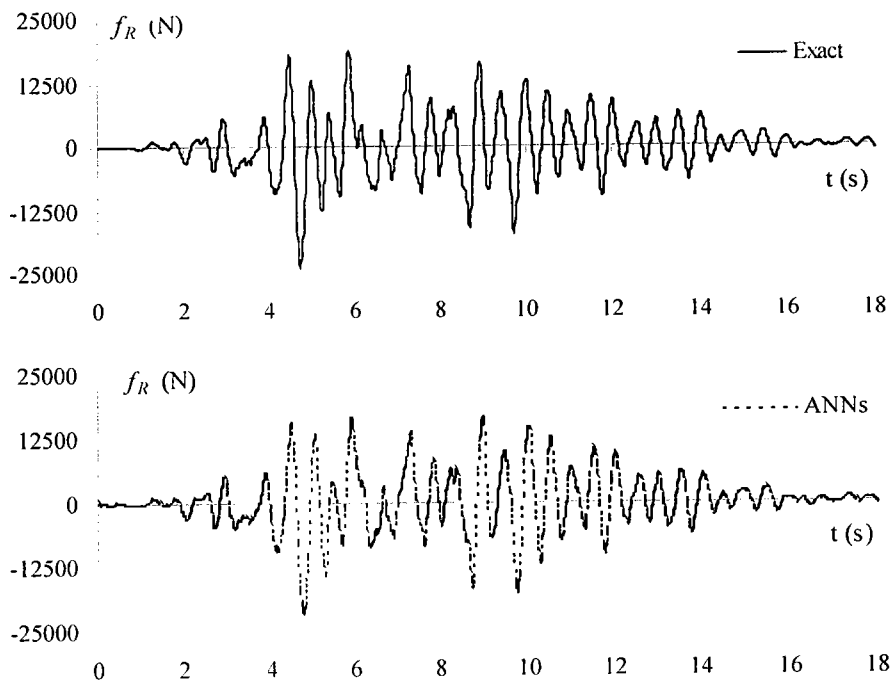


Fig. 4.22 Restoring force resulting from the second ground acceleration A_{g2}

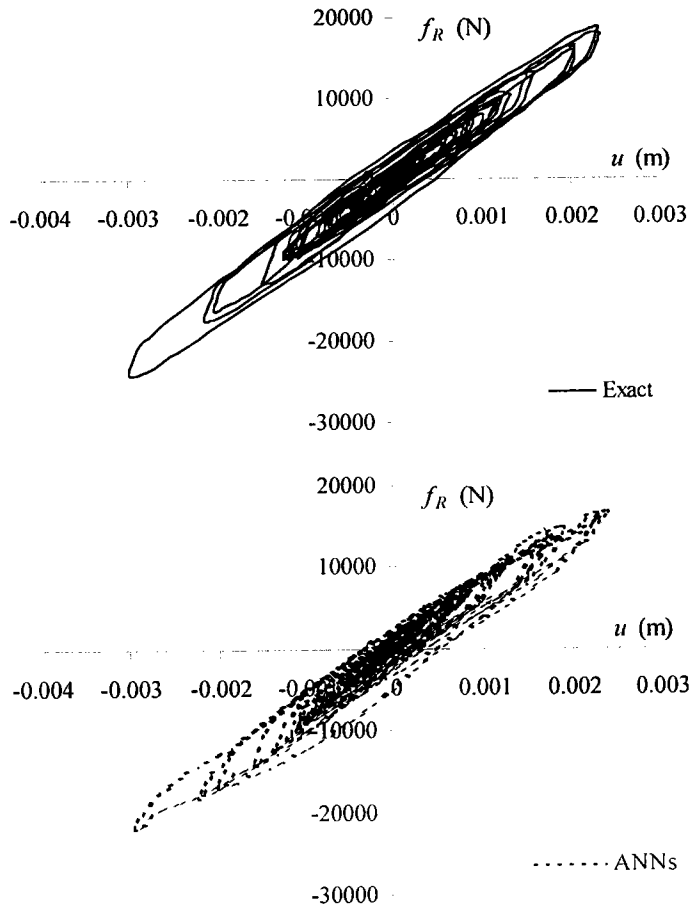


Fig. 4.23 Restoring force-Displacement Relation from the second ground acceleration A_{g2}

3) Case of $\alpha = 0.1$ and unknown damping

Consider Eq. (4.8),

$$m \ddot{u} + c \dot{u} + \alpha k_1 u + (1 - \alpha) k_1 Z = -m A_g. \quad (4.26)$$

Here the restoring force,

$$f_R = c \dot{u} + \alpha k_1 u + (1 - \alpha) k_1 Z. \quad (4.27)$$

The hybrid discrete-ANNs system in the case of unknown damping can be written as:

$$m \ddot{u} + f_{ANN} = -m A_g. \quad (4.28)$$

The system parameters are shown in the following table.

Table 4.5 Parameters used in Clough-Johnston hysteretic model ($\alpha = 0.1$)

Parameter (unit)		Value
m	kg	50,000
c	Ns/m	65,900
k_l	N/m	24,200,000
Z_Y	m	0.00015
α		0.1
D_o	m	-0.00114
Z_o	m	0
u_0	m	0
\dot{u}_0	m/s	0
\ddot{u}_0	m/s ²	0

3.1) Selection a network input

As described in section 3.4, Nonlinear restoring force of Non-conservative system was predicted dependent on past response history. From Eq. (3.12) the input parameters for predicting nonlinear restoring force are

$$y = [u, u_{t-1}, u_{t-2}, \dot{u}, \dot{u}_{t-1}, \dot{u}_{t-2}, f_{R,t-1}, f_{R,t-2}]. \quad (4.29)$$

3.2) Training the network

The first earthquake record, A_{gl} , is used as the training data set. The total duration for training time histories is 20 seconds from which the input values are extracted from the time histories and fed into the network at every 0.01-second.

From parametric study, the two hidden layer neural network and 10-10 hidden neurons yield satisfactory results. The learning rate is 0.5 and training for 2,000 epoch. The corresponding optimal weights for this duffing system are given in Appendix G.

The exact results, or computed from Eq. (4.26), is compared with those from ANNs, as shown in Figs. 4.24, 4.25 and 4.26.

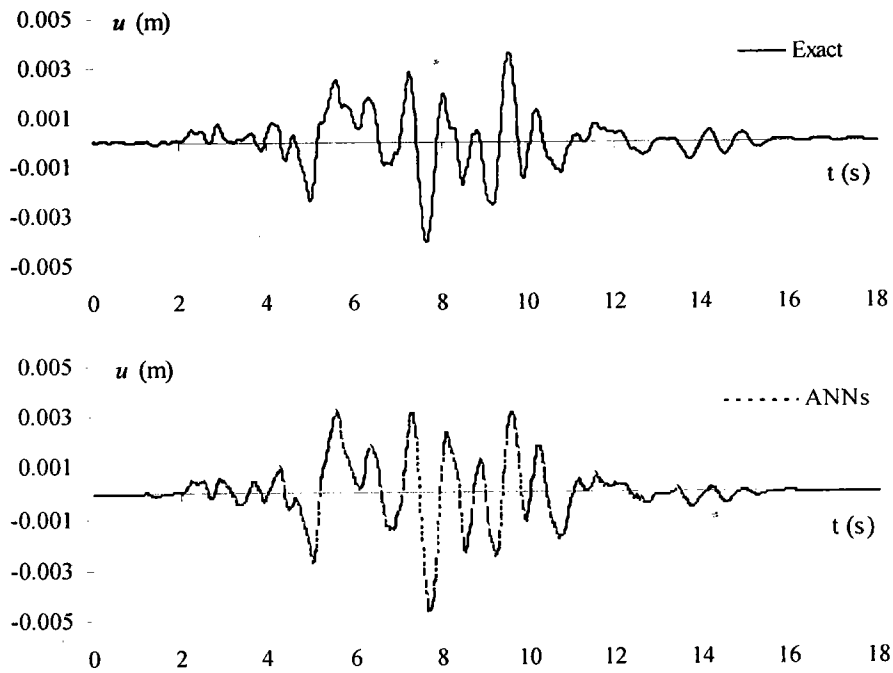


Fig. 4.24 Displacement resulting from the first ground acceleration A_{g1}

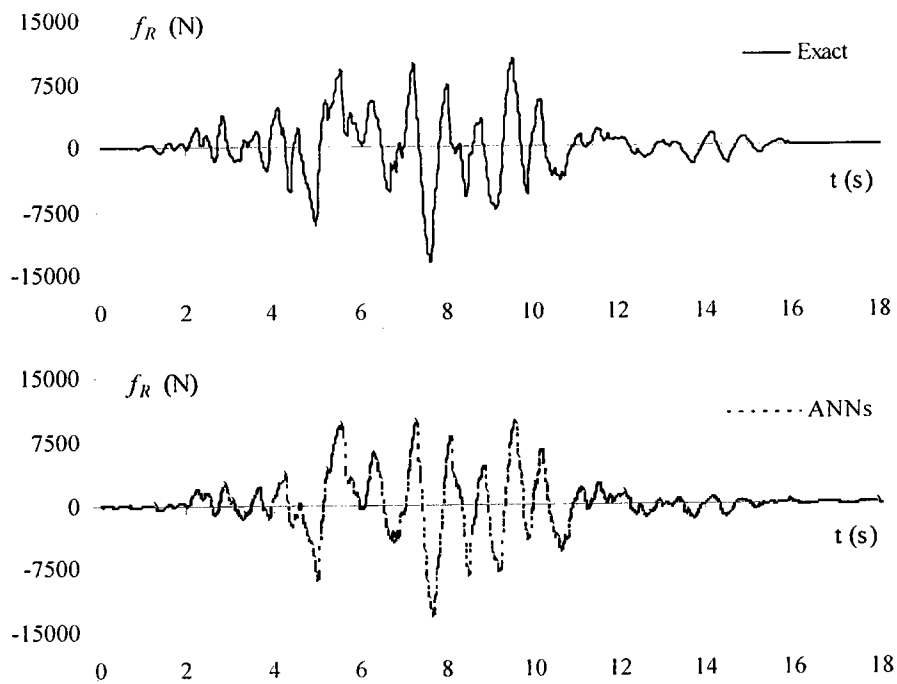


Fig. 4.25 Restoring force resulting from the first ground acceleration A_{g1}

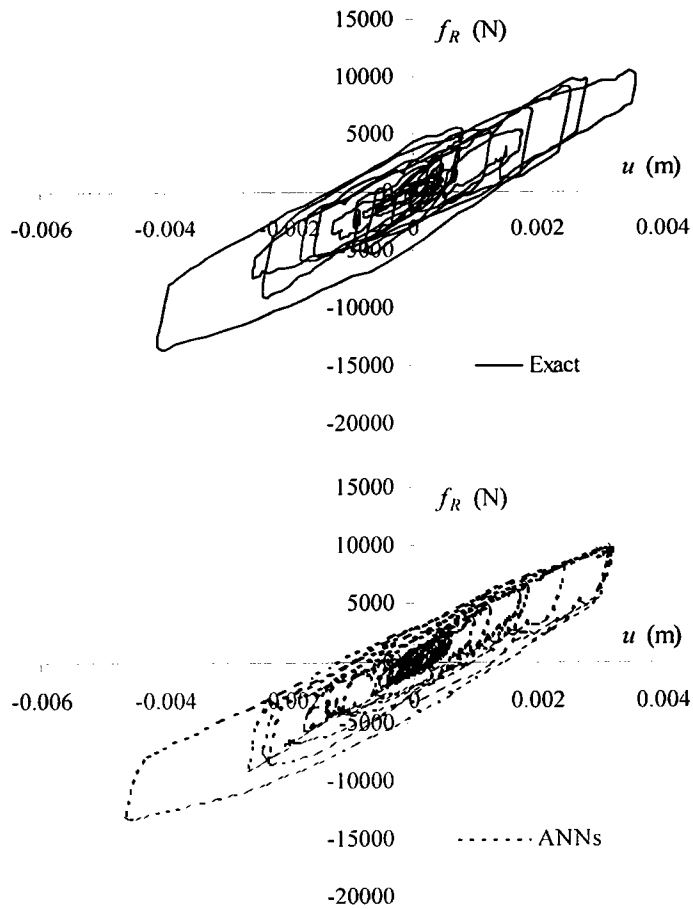


Fig. 4.26 Restoring force-Displacement relation from the first ground acceleration A_{g1}

3.3) Testing the trained network

The predicted responses of this system from the trained ANN using the second ground acceleration record, A_{g2} are shown in Figs. 4.27 – 4.29.

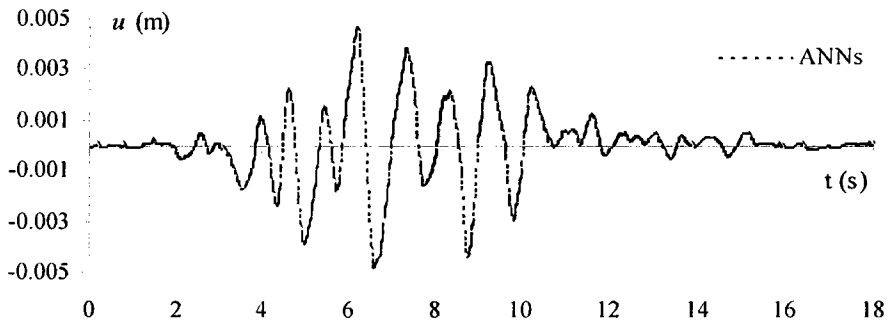
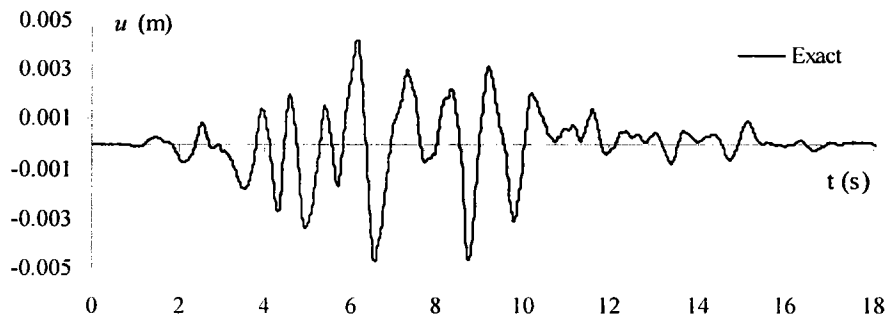


Fig. 4.27 Displacement resulting from the second ground acceleration A_{g2}

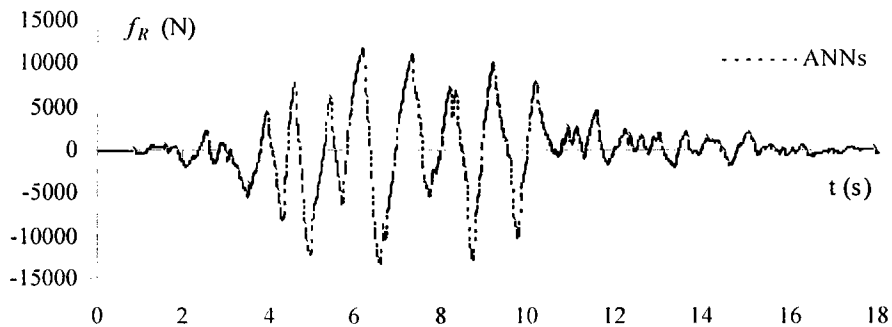
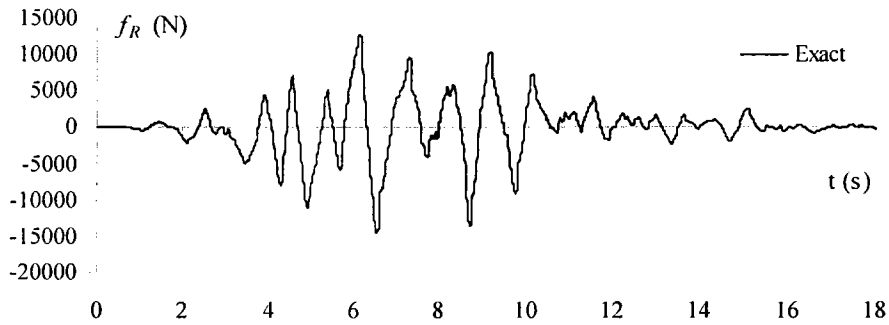


Fig. 4.28 Restoring force resulting from the second ground acceleration A_{g2}

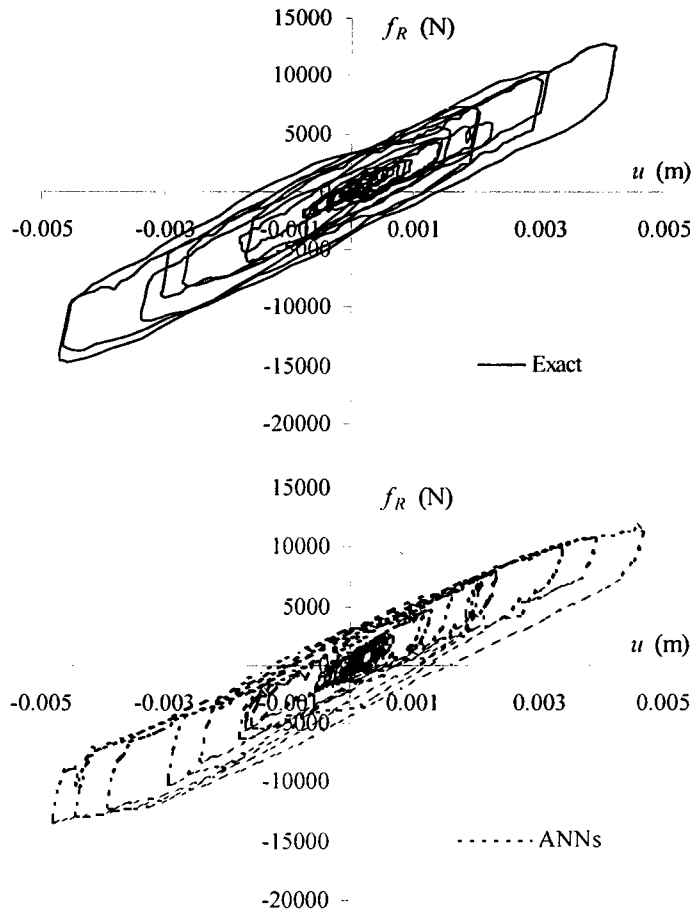


Fig. 4.29 Restoring force-Displacement relation from the second ground acceleration A_{g2}

4.5.2 Extended Bouc-Wen-Barber-Noori hysteretic system

To investigate further the applicability potential, the next example considers the Extended Bouc-Wen-Barber-Noori (EBWBN) hysteretic model (Foliente et al. 1996). This model accounts for the strength degradation, the stiffness degradation, and the generalized pinching behavior. When appropriately choosing the model parameters, the EBWBN can model the behaviors of various structural elements. The equation of motion for an EBWBN system under the base excitation A_g is

$$m \ddot{u} + c \dot{u} + \alpha k_1 u + (1 - \alpha) k_1 Z = -m A_g \quad (4.30)$$

$$\dot{Z} = h(Z) \left\{ \frac{\dot{u} - v(\beta |\dot{u}| |Z|^{r-1} Z + \gamma \dot{u} |Z|^r)}{\eta} \right\} \quad (4.31)$$

$$v(\varepsilon) = 1.0 + \delta_v \varepsilon \quad (4.32)$$

$$\eta(\varepsilon) = 1.0 + \delta_\eta \varepsilon \quad (4.33)$$

$$\varepsilon = (1 - \alpha) k \int_{t_0}^{t'} Z \dot{u} dt \quad (4.34)$$

$$h(Z) = 1.0 - \zeta_1 \exp[-(Z \operatorname{sgn}(\dot{u}) - dZ)^2 / \zeta_2^2] \quad (4.35)$$

$$Z_u = \left[\frac{1}{v(\beta + \gamma)} \right]^{1/r} \quad (4.36)$$

$$\zeta_1(\varepsilon) = \zeta_{1,0} [1 - \exp(-s\varepsilon)] \quad (4.37)$$

$$\zeta_2(\varepsilon) = (\psi_0 + \delta_\psi \varepsilon)(\lambda + \zeta_1) \quad (4.38)$$

where β, γ, r are the hysteretic shape parameters (if $r = \infty$, the elasto plastic hysteretic case is obtained), v, η are the strength and the stiffness degradation parameters, respectively (if $v = \eta = 1.0$, the model does not degrade), and $h(Z)$ is the pinching function (if $h(Z) = 1.0$ the model does not pinch). The absorbed hysteretic energy, ε , which controls pinching, strength and stiffness degradation. ζ is a pinching parameter controlling the severity and rate of pinching. ψ_0 is the pinching parameter. s is a parameter controlling the rate of initial drop in slope. λ is pinching parameter.

From Eq. (4.30), α determine the effect of elasticity as well as CJ model. Then, two cases of α are considered here, namely $\alpha = 0.3$ and 0.1 respectively. Only unknown damping cases are considered. This case reflects the real situations that the damping force may not be known. The initial condition of dynamical system above can represent as:

$$u(0) = u_0, \dot{u}(0) = \dot{u}_0, \ddot{u}(0) = \ddot{u}_0 \quad (4.39)$$

$$Z(0) = Z_0. \quad (4.40)$$

Two seismic records are utilized consecutively. The first record is the Scaled EI-Centro ground acceleration A_{g3} . This record is used for generating the training data set. The second record is A_{g1} , which is assumed taking place 9 sec. after the first earthquake. In this system, the training ground acceleration characteristic, A_{g3} , is different from testing, A_{g1} , to check the generality of ANNs when subject to different input response spectra.

1) Case of $\alpha = 0.3$ and unknown damping

Consider equation of motion, Eq. (4.30),

$$m \ddot{u} + c \dot{u} + \alpha k_1 u + (1 - \alpha) k_1 Z = -m A_g. \quad (4.41)$$

Here the Restoring Force.

$$f_R = c\dot{u} + \alpha k_1 u + (1-\alpha)k_1 Z, \quad (4.42)$$

is assumed as unknown and modeled by ANNs. That is

$$m \ddot{u} + f_{ANN} = -m A_R. \quad (4.43)$$

Table 4.6 shows parameters that used in this example $\alpha = 0.3$.

Table 4.6 Parameters used in EBWBN hysteretic model ($\alpha = 0.3$)

Parameter (unit)		Value
m	kg	10,000
c	Ns/m	50,000
k_1	N/m	1,000,000
α		0.3
β		1.5
γ		-0.5
r		1
s		2
d		0.2
δ_v		0.4
δ_n		0.9
δ_ψ		0.05
ζ_{10}		0.8
ψ_0		0.8
λ		1.5
u_0	m	0
\dot{u}_0	m/s	0
\ddot{u}_0	m/s ²	0
Z_0	m	0

1.1) Selection a network inputs

As same as CJ hysteretic system, the EBWBN hysteretic system is using the same input parameters. From Eq. (3.12) the input parameters for predicting nonlinear non-conservative restoring force are

$$\mathbf{y} = [u_t \ u_{t-1} \ u_{t-2} \ \dot{u}_t \ \dot{u}_{t-1} \ \dot{u}_{t-2} \ f_{R,t-1} \ f_{R,t-2}]. \quad (4.44)$$

1.2) Training the network

The Scaled EI-Centro seismic record, A_{g3} , is used as the training data set. The total duration for training time histories is 20 seconds from which the input values are extracted from the time histories and fed into the network at every 0.01-second.

From parametric study, the two hidden layer neural network and 13-13 hidden neurons yield satisfactory results. The learning rate is 0.1 and training for 6,000 epoch. The corresponding optimal weights for this duffing system are given in Appendix H.

The exact results, or computed from Eq. (4.41), is compared with those from ANNs, as shown in Figs. 4.30, 4.31 and 4.32.

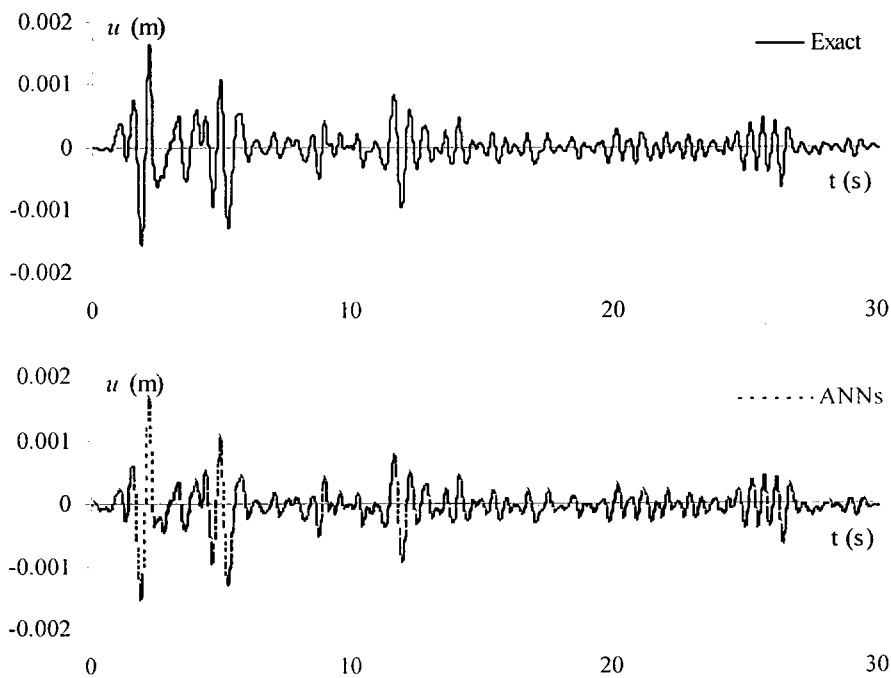


Fig. 4.30 Displacement resulting from the Scaled EI-Centro ground acceleration A_{g3}

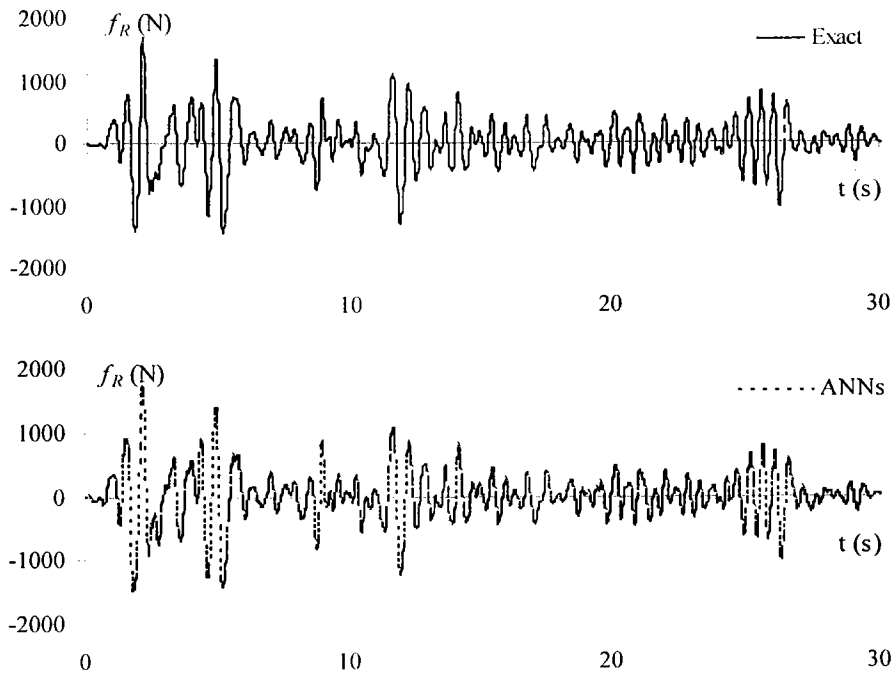


Fig. 4.31 Restoring force resulting from the Scaled EI-Centro ground acceleration A_{g3}

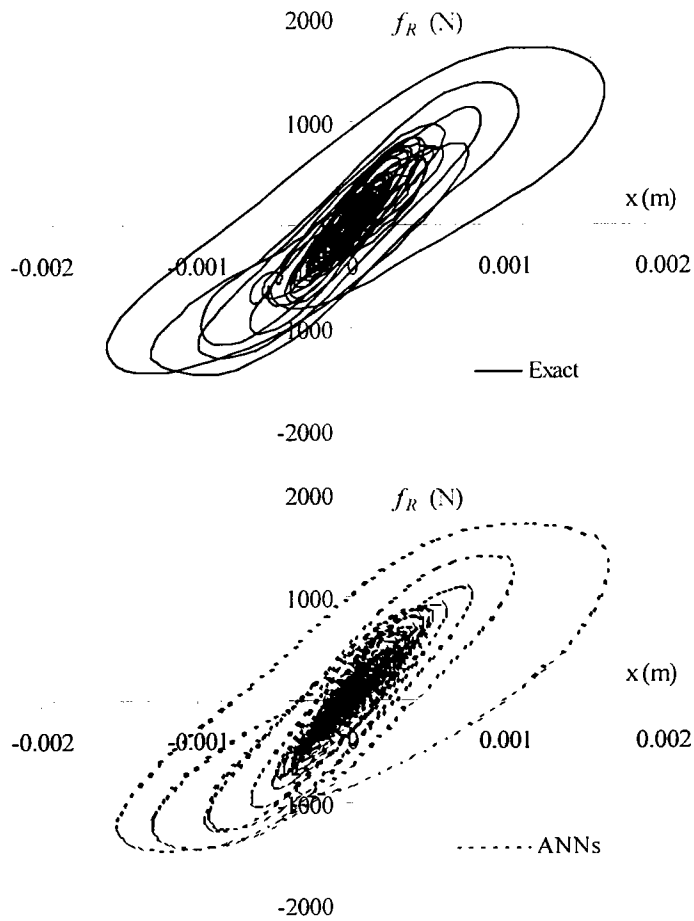


Fig. 4.32 Restoring force-Displacement relation from the Scaled EI-Centro ground acceleration A_{g3}

1.3) Testing the trained network

The predicting responses of this system from the trained ANN using the first ground acceleration record, A_{g1} , are shown in Figs. 4.33 – 4.35. The testing process by using A_{g1} also does using the initial condition from the previous seismic record, A_{g3} , from the consideration of path-dependent behavior of hysteretic system.

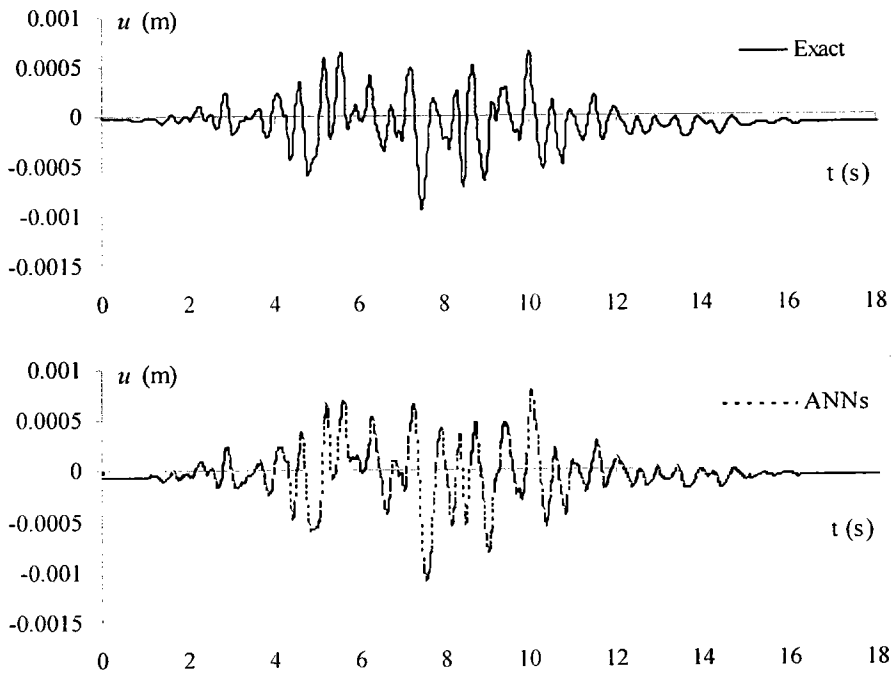


Fig. 4.33 Displacement resulting from the first ground acceleration A_{g1}

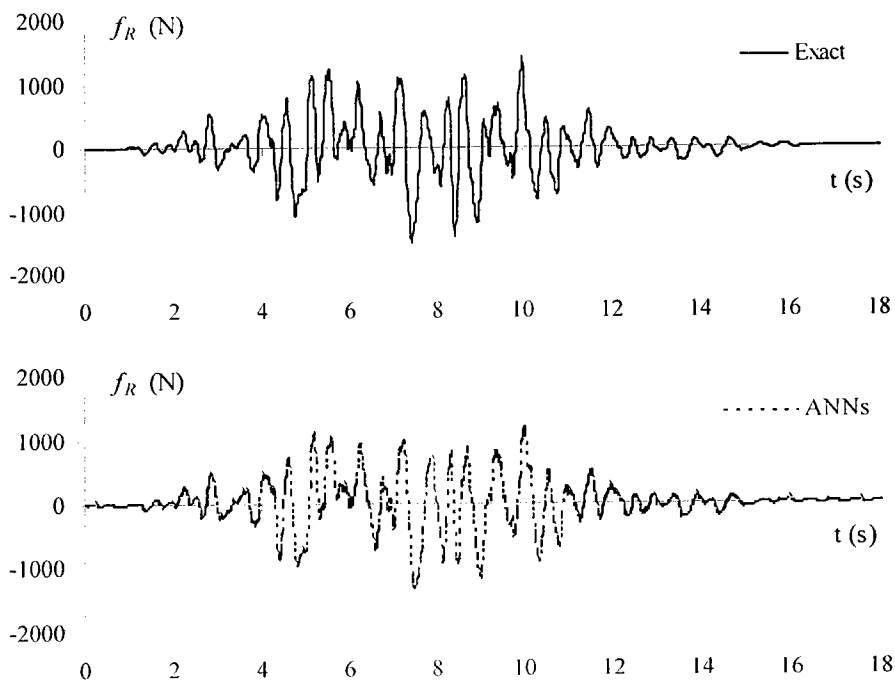


Fig. 4.34 Restoring force resulting from the first ground acceleration A_{g1}

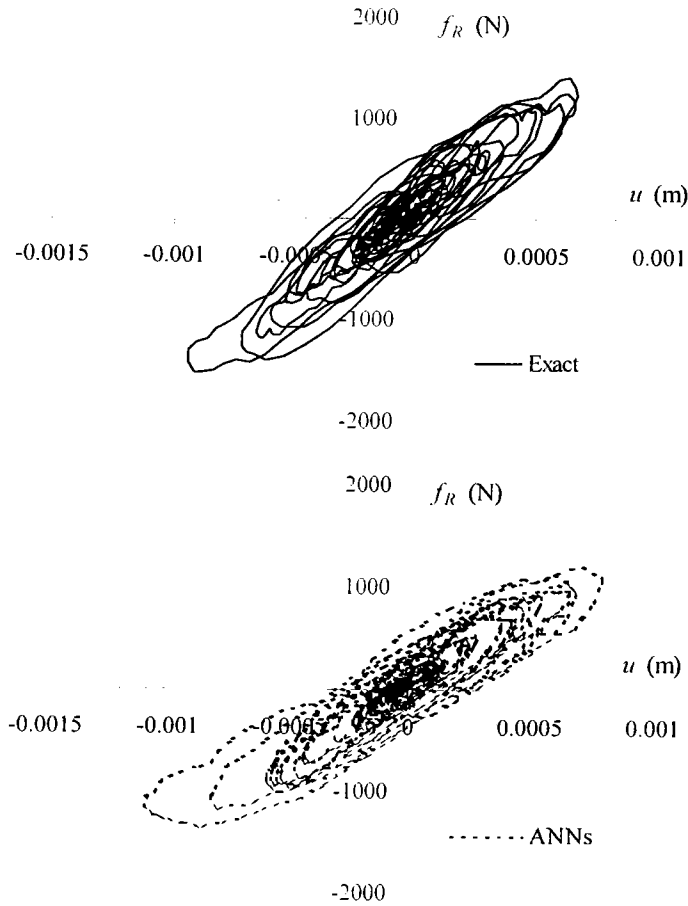


Fig. 4.35 Restoring force-Displacement relation from the first ground acceleration A_{g1}

2) Case of $\alpha = 0.1$ and unknown damping

The equation of motion of EBWBN hysteretic system, Eq. (4.30), is repeated:

$$m \ddot{u} + c \dot{u} + \alpha k_1 u + (1 - \alpha) k_1 Z = -m A_g \quad (4.45)$$

The Restoring Force is

$$f_R = c \dot{u} + \alpha k_1 u + (1 - \alpha) k_1 Z \quad (4.46)$$

In verification process, the restoring force value, f_R , will undertake by network (f_{ANN}). Then, the Eq. (4.45) is change to be:

$$m \ddot{u} + f_{ANN} = -m A_g \quad (4.47)$$

Table 4.7 shows parameters that used in this example $\alpha = 0.1$ with unknown damping.

Table 4.7 Parameters used in EBWBN hysteretic model ($\alpha = 0.1$)

Parameter (unit)		Value
m	kg	10,000
c	Ns/m	50,000
k_l	N/m	1,000,000
α		0.1
β		1.5
γ		-0.5
r		1
s		2
d		0.2
δ_v		0.4
δ_η		0.9
δ_ψ		0.05
ζ_{10}		0.8
ψ_0		0.8
λ		1.5
u_0	m	0
\dot{u}_0	m/s	0
\ddot{u}_0	m/s ²	0
Z_0	m	0

2.1) Selection a network inputs

As same as CJ hysteretic system, the EBWBN hysteretic system is using the same input parameters. From Eq. (3.12) the input parameters for predicting nonlinear non-conservative restoring force are

$$y = [u_t \ u_{t-1} \ u_{t-2} \ \dot{u}_t \ \dot{u}_{t-1} \ \dot{u}_{t-2} \ f_{R,t-1} \ f_{R,t-2}]. \quad (4.48)$$

In addition, to study the effect of input neurons in predicting restoring force value, the increasing of time delay step is investigated by apply the same variable of neurons as in the previous hysteretic system but increasing delay for 3-time step i.e.,

$$y = [u_t \ u_{t-1} \ u_{t-2} \ u_{t-3} \ \dot{u}_t \ \dot{u}_{t-1} \ \dot{u}_{t-2} \ \dot{u}_{t-3} \ f_{R,t-1} \ f_{R,t-2} \ f_{R,t-3}], \quad (4.49)$$

for predict $f_{R,t}$. This new input neuron will compare with the 2-time delay step for the case of unknown damping case for α equal to 0.1.

2.2) Training the network

The Scaled EI-Centro earthquake record, A_{g3} , is used as the training data set. The training data are using simulated response of A_{g3} for 20 seconds and fed into the network every 0.01-second.

From parametric study, The type of input nodes delay for 2-time delay step yield the best result than 3-time delay step case and the two hidden layer neural network with 13-13 hidden neurons yields satisfactory results. The learning rate is 0.3 and training for 2000 epochs. The corresponding optimal weights for this system are given in Appendix I.

The exact results, or computed from Eq. (4.45), is compared with those from ANNs, as shown in Figs. 4.36, 4.37 and 4.38.

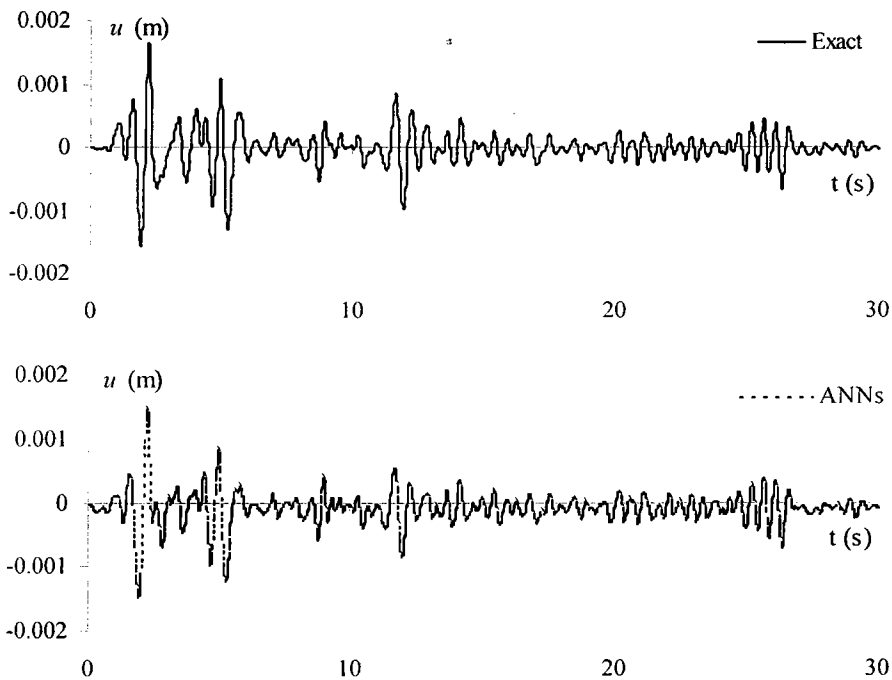


Fig. 4.36 Displacement resulting from the Scaled EI-Centro ground acceleration A_{g3}

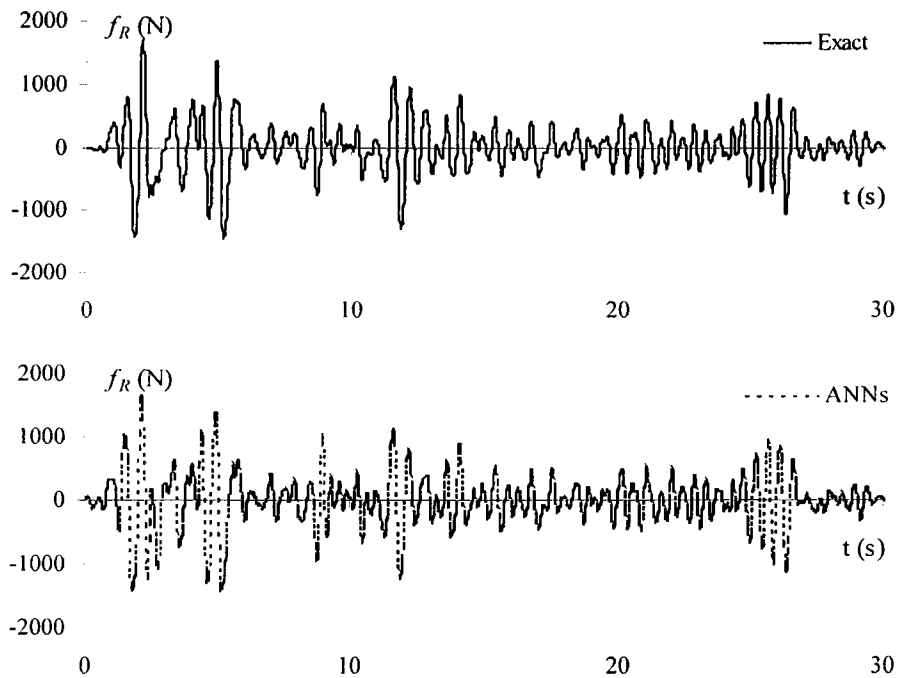


Fig. 4.37 Restoring force resulting from the Scaled EI-Centro ground acceleration A_{g3}

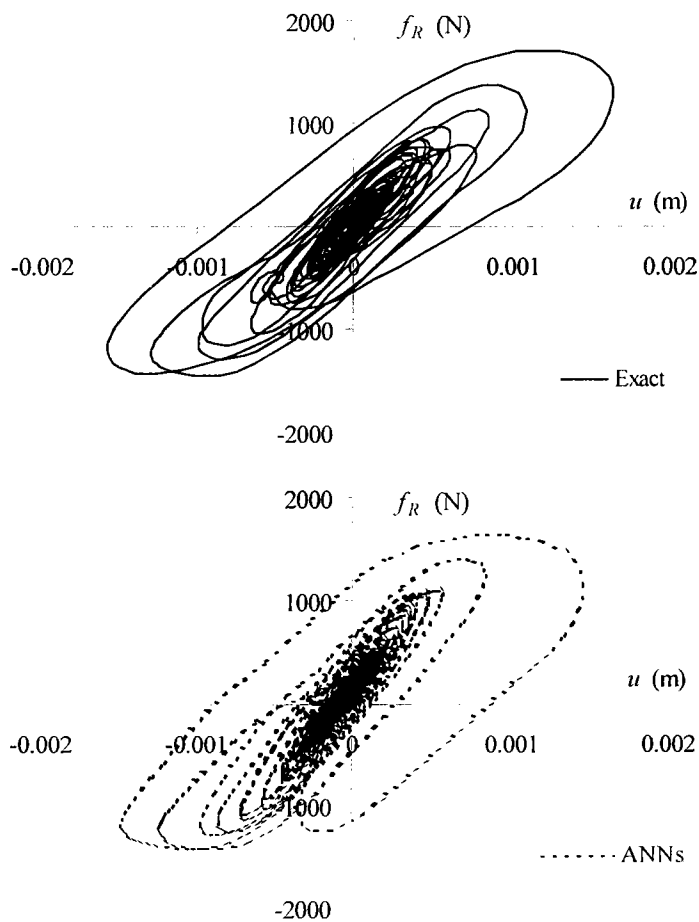


Fig. 4.38 Restoring force-Displacement relation from the Scaled EI-Centro ground acceleration A_{g3}

2.3) Testing the trained network

The predicting responses of this system by ANN with first ground acceleration record, A_{g1} , are shown in Figs. 4.39 – 4.41. The testing process by using A_{g1} also does using the initial condition from the previous seismic record, A_{g3} , from the consideration of path-dependent behavior of hysteretic system.

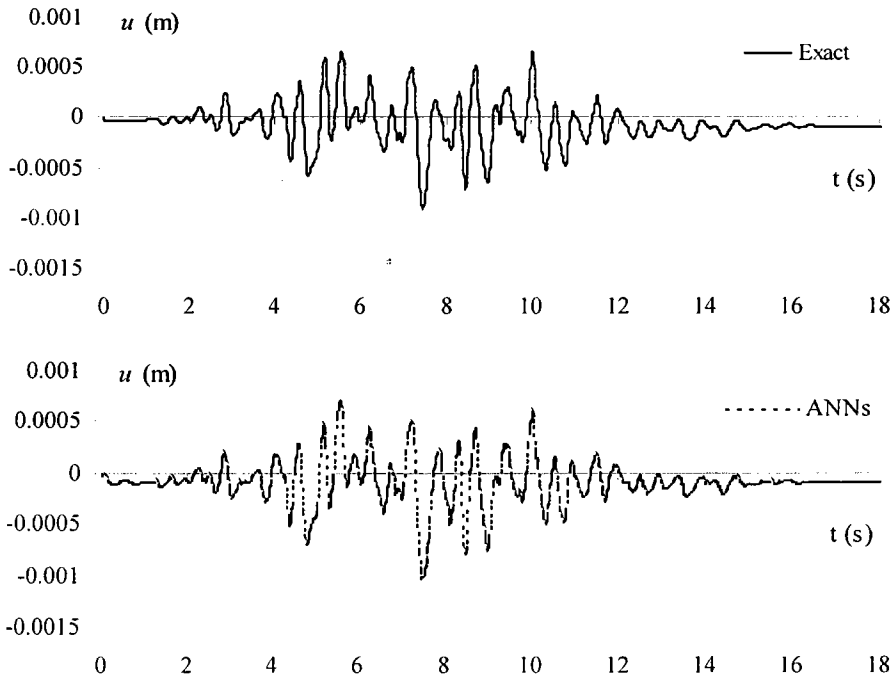


Fig. 4.39 Displacement resulting from the first ground acceleration A_{g1}

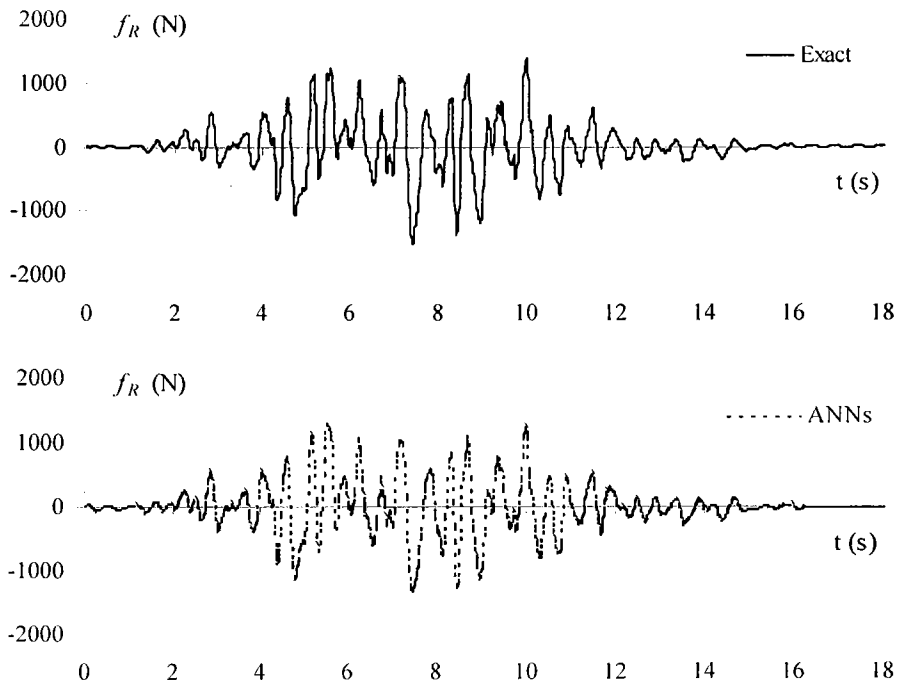


Fig. 4.40 Restoring force resulting from the first ground acceleration A_{g1}

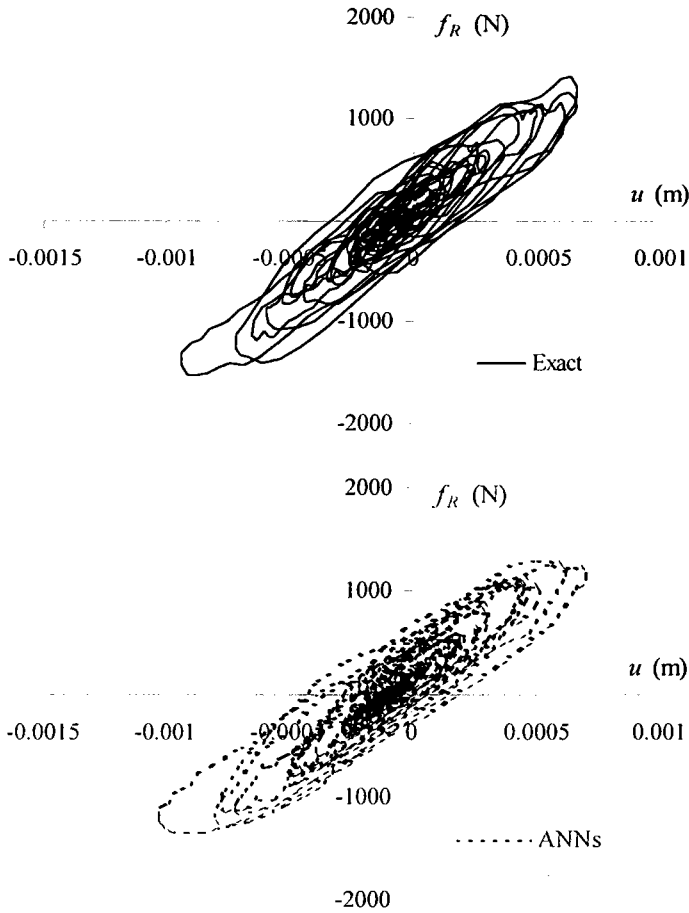


Fig. 4.41 Restoring force-Displacement relation from the first ground acceleration A_{g1}

4.6 Nonlinear Conservative MDOF System

A 5-story shear-beam building is study in this case in which the restoring force in the fourth-floor is modeled by ANNs. The building is subjected to ground acceleration, A_{g1} . The spring force due to the stiffness of the columns in each floor is described by

$$f_s(x) = k_1x + k_2x^3 \quad (4.50)$$

in which k_1 and k_2 are system parameters and equal to 100,000 and 10,000 N/m respectively, and x is the relative floor-displacement. The equation of motion of the hybrid FE-ANNs model, when \mathbf{u} is the vector of floor displacements, can be derived as

$$m\ddot{\mathbf{u}} + c\dot{\mathbf{u}} + \mathbf{f}_{NL} + \mathbf{f}_{ANN} = -\mathbf{m}\Lambda A_G \quad (4.51)$$

$$\Lambda = [1 \quad 1 \quad 1 \quad 1 \quad 1]^T \quad (4.52)$$

where

$$\mathbf{m} = \begin{bmatrix} m_1 & 0 & 0 & 0 & 0 \\ 0 & m_2 & 0 & 0 & 0 \\ 0 & 0 & m_3 & 0 & 0 \\ 0 & 0 & 0 & m_4 & 0 \\ 0 & 0 & 0 & 0 & m_5 \end{bmatrix} \quad (4.53)$$

in which $m_1 = m_2 = m_3 = m_4 = m_5 = 150,000$ kg

$$\mathbf{c} = \begin{bmatrix} c_1 + c_2 & -c_2 & 0 & 0 & 0 \\ -c_2 & c_2 + c_3 & -c_3 & 0 & 0 \\ 0 & -c_3 & c_3 + c_4 & -c_4 & 0 \\ 0 & 0 & -c_4 & c_4 + c_5 & -c_5 \\ 0 & 0 & 0 & -c_5 & c_5 \end{bmatrix} \quad (4.54)$$

in which $c_1 = c_2 = c_3 = c_5 = 65,900$ Ns/m. It is assumed in this situation that c_4 is also not known. The spring forces due to the stiffness of the columns in all floors except that in the fourth floor build up f_{NL} , i.e.

$$\mathbf{f}_{NL} = \begin{bmatrix} f_{s1} - f_{s2} \\ f_{s2} - f_{s3} \\ f_{s3} - 0 \\ 0 - f_{s5} \\ f_{s5} \end{bmatrix} \quad (4.55)$$

The missing restoring force at the fourth-floor level then appears in f_{ANN} ,

$$\mathbf{f}_{ANN} = [0 \quad 0 \quad -f_{ANN} \quad f_{ANN} \quad 0]^T \quad (4.56)$$

in which f_{ANN} is a functional representation of an ANN model, as introduced in Eq. (3.5).

Two seismic records are utilized consecutively. The first record is the first earthquake ground acceleration A_{g1} . This record is used for generating the training data set. The second record is A_{g2} , which is assumed taking place 19 seconds after the first earthquake.

1) Selection a network inputs

Eq. (4.50) give the individual functional relationship for nonlinear spring force and displacement

$$f_{ANN} = ANN(x_4, \dot{x}_4) \quad (4.57)$$

where

$$x_4 = u_4 - u_3. \quad (4.58)$$

The network architecture for predicting nonlinear restoring force of fourth floor is shown in Fig. 4.42.

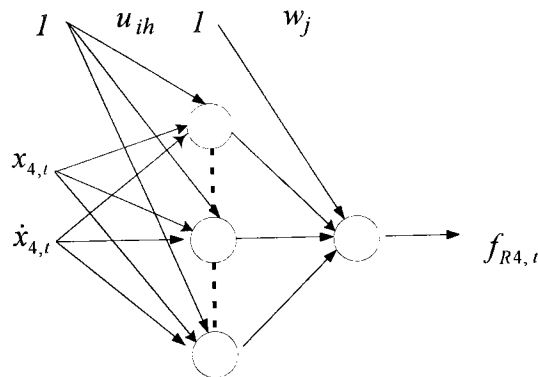


Fig. 4.42 Architecture of ANNs for modeling of nonlinear conservative restoring force

2) Training the network

The first earthquake record, A_{g1} , is used as the training data set. The training data are using simulated response of A_{g1} for 20 seconds and fed into the network every 0.01-second.

From parametric study, the one hidden layer neural network with 8 hidden neurons yields satisfactory results. The corresponding optimal weights for this system are given in Appendix J.

The exact results, or computed from Eq. (4.51), is compared with those from ANNs, as shown in Figs. 4.43 to 4.46.

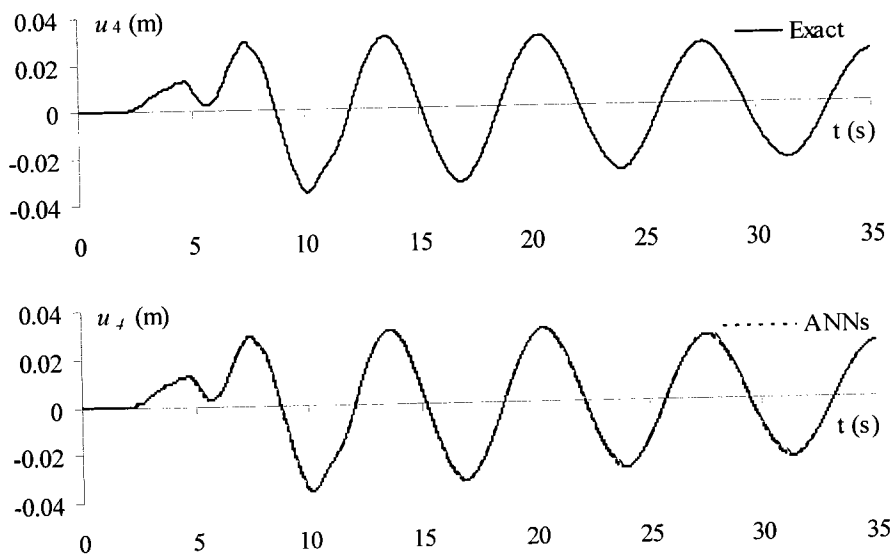


Fig. 4.43 Displacement of fourth floor slab resulting from the first ground acceleration A_{g1}

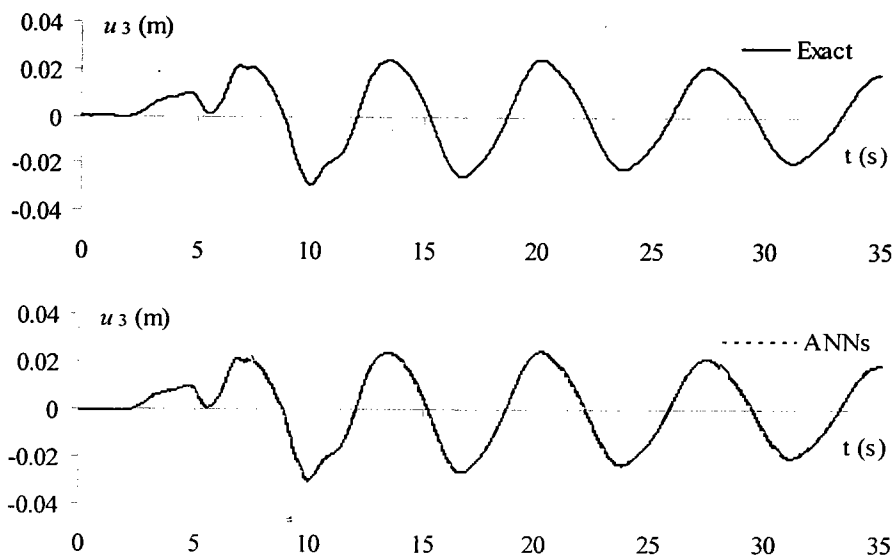


Fig. 4.44 Displacement of third floor slab resulting from the first ground acceleration A_{g1}

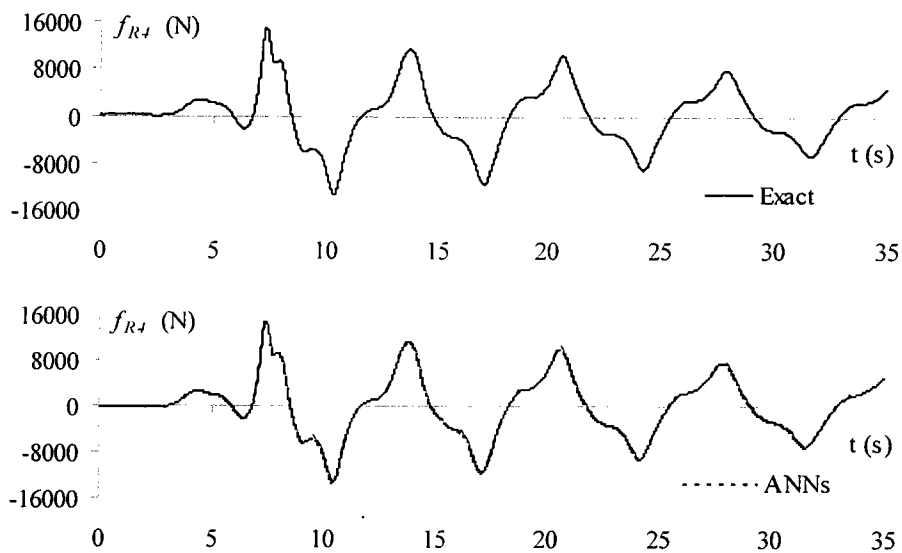


Fig. 4.45 Restoring force of fourth floor slab resulting from the first ground acceleration A_{g1}

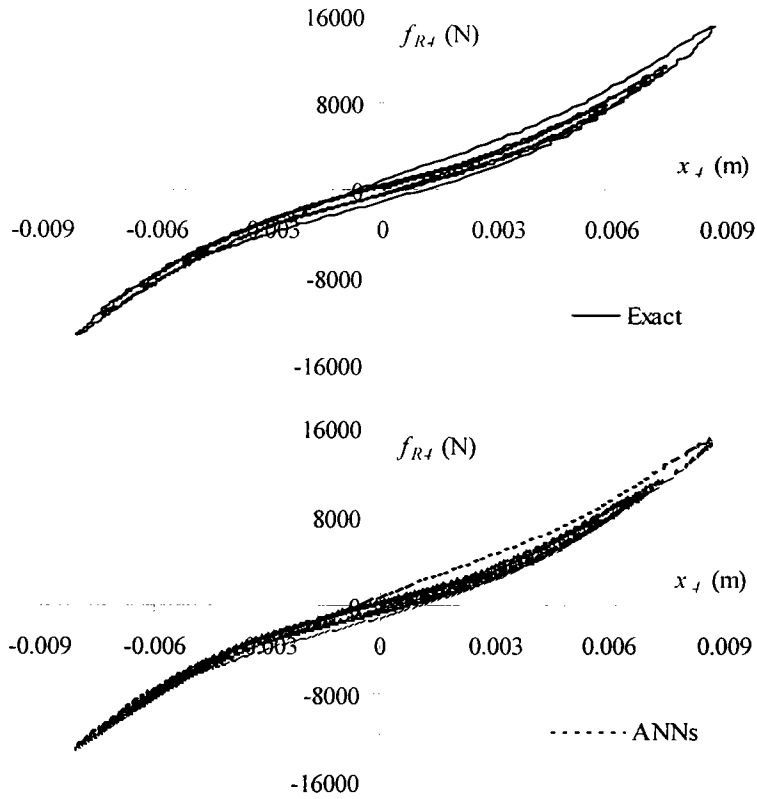


Fig. 4.46 Restoring force-Displacement relation of fourth floor slab from the first ground acceleration A_{g1}

3) Testing the trained network

The predicting responses of this system by ANN with second ground acceleration record, A_{g2} , are shown in Figs. 4.47 – 4.50.

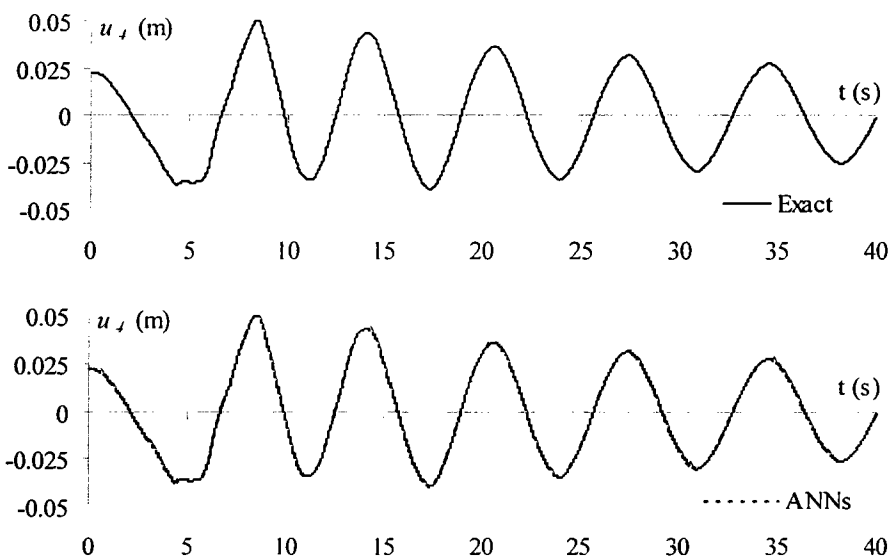


Fig. 4.47 Displacement of fourth floor slab resulting from the second ground acceleration A_{g2}

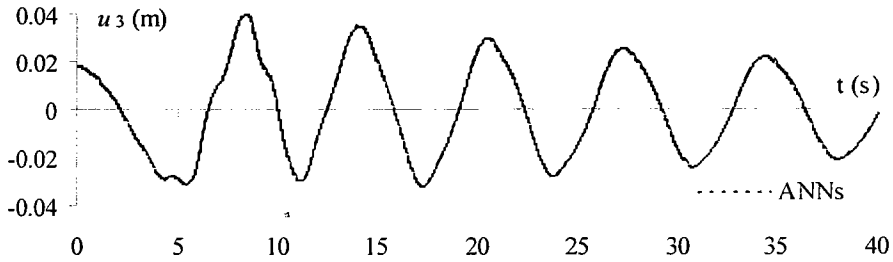
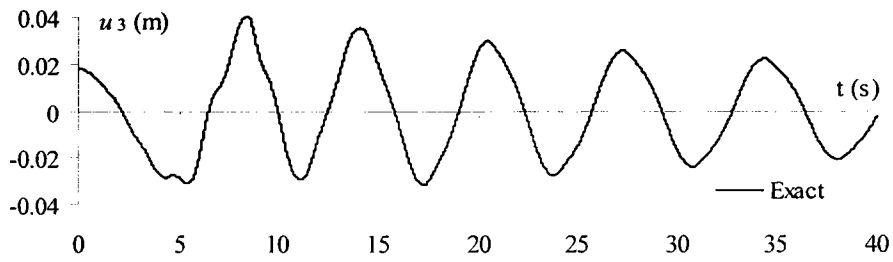


Fig. 4.48 Displacement of third floor slab resulting from the second ground acceleration A_{g2}

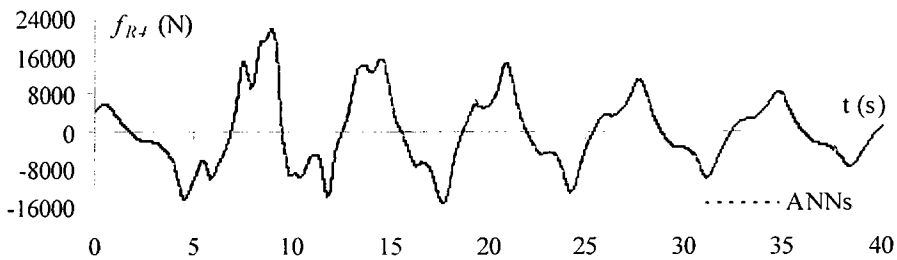
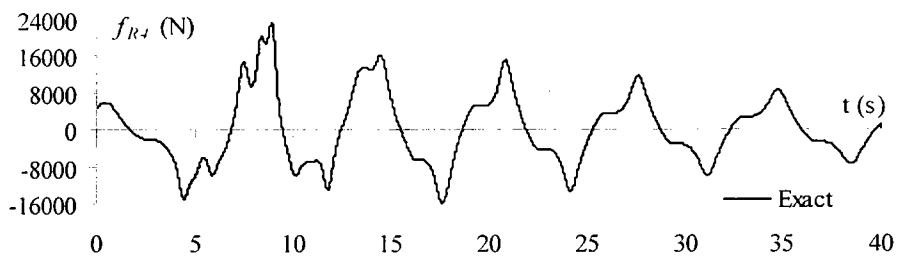


Fig. 4.49 Restoring force of fourth floor slab resulting from the second ground acceleration A_{g2}

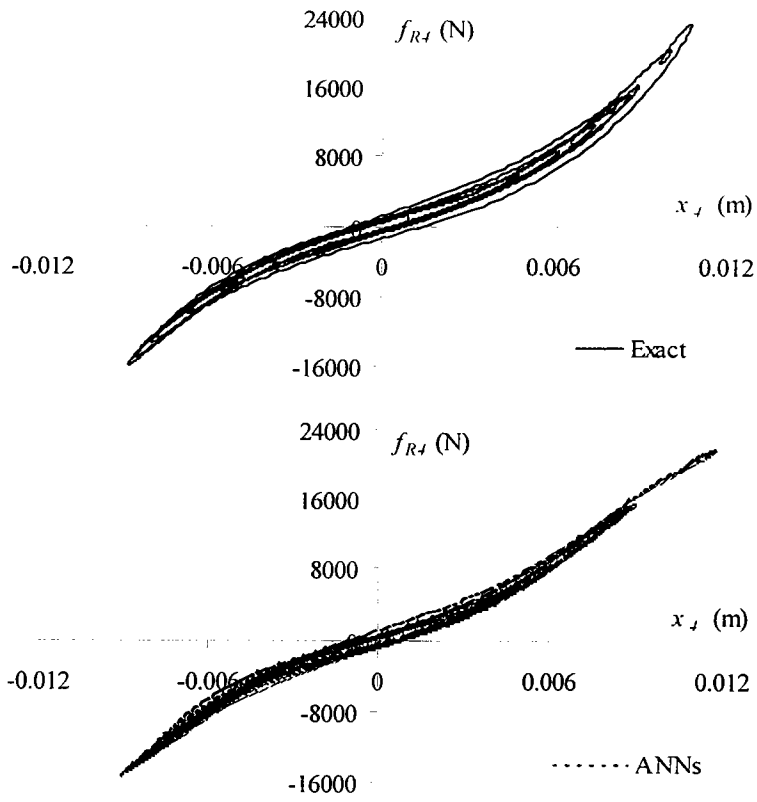


Fig. 4.50 Restoring force-Displacement relation of fourth floor slab from the second ground acceleration A_{g2}